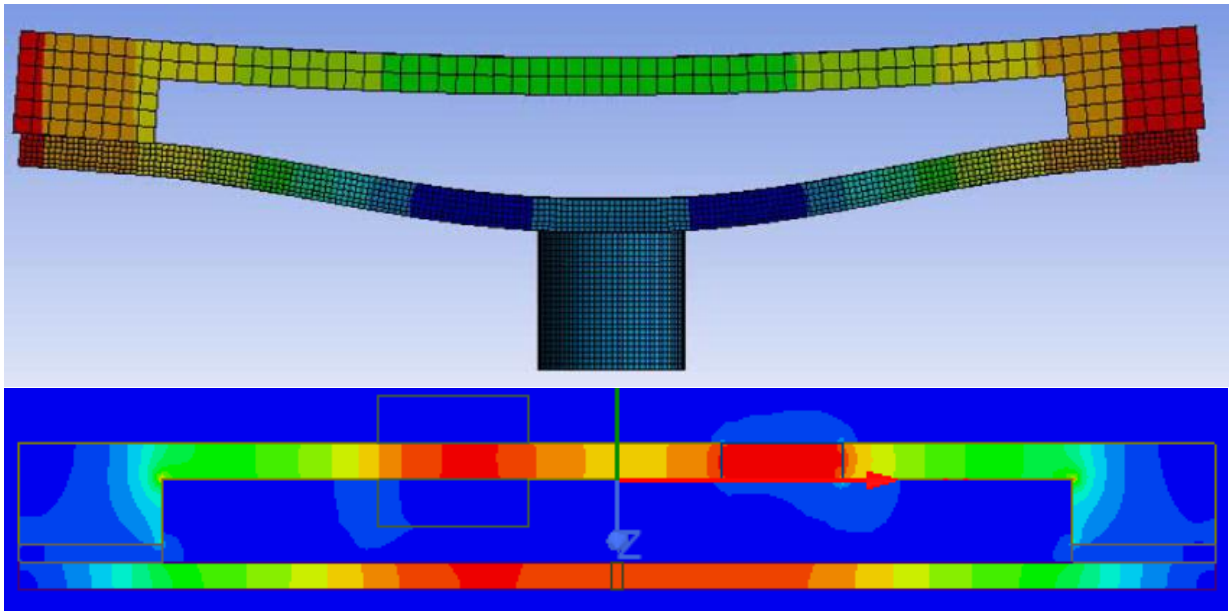

Novel Design of Transducer for Bone Conduction Use

Department of Electrical Engineering together with Cochlear Bone Anchored Solutions AB.

UTKU AYVAZ

Department of Electrical Engineering
CHALMERS UNIVERSITY OF TECHNOLOGY
Master's thesis EENX60
Gothenburg, Sweden 2022
www.chalmers.se

MASTER'S THESIS 2022

Novel Design of Transducer for Bone Conduction Use

By: Utku Ayvaz

CHALMERS
UNIVERSITY OF TECHNOLOGY

Department of Electrical Engineering

Division of Signal Processing and Biomedical Engineering

Chalmers University of Technology

Gothenburg, Sweden 2022

Novel Design of Transducer for Bone Conduction Use

Utku Ayvaz

Supervisor: Dan Nyström, Cochlear Bone Anchored Solutions AB

Examiner: Associate Professor Sabine Reinfeldt, Department of Electrical Engineering

Master's Thesis 2022: EENX60
Department of Electrical Engineering
Chalmers University of Technology
SE-412 96 Gothenburg
Telephone +46 31 772 1000

Cover: A representation of mechanical and electromagnetic operations of the transducer during simulations.

Novel Design of Transducer for Bone Conduction Use

Department of Electrical Engineering

Gothenburg, Sweden 2022

Abstract

Hearing losses are worldwide acknowledged health problems affecting overall life quality of suffering patients. Different types of hearing aids were developed to rehabilitate and treat people suffering from hearing traumas. One such type of hearing aid is the bone conduction (BC) hearing aid, which is helpful for indicated patients. BC has been used for many decades in hearing aids, and there are now several implantable versions. These hearing aids transmit the sound through the skull bones to the inner part of the ear, bypassing the outer and middle parts. BC hearing aids are essentially designed with a transducer principle. This principle transforms electrical signals into mechanical vibrations. The main objective of this project is to find a possible magnetostrictive transducer design and provide optimized data to build a possible magnetostrictive transducer for bone conduction use.

Ferromagnetic material options were investigated to replace piezoelectric ceramics that are frequently used in BC hearing implants. According to the literature review, the ferromagnetic alloys Terfenol D, Galfenol, and Metglas 2714A® were identified as possible materials for bender in the transducer. The ANSYS® Mechanical and Electronics environment was chosen for simulations and testing. Mechanical dimensions were simulated and optimized regarding size and resonance frequency, similar to existing bone conduction transducers. As a result of modal and harmonic response analysis, it was found that 0.3 and 0.4 mm for Metglas 2714A®, and 0.4 and 0.5 mm for Galfenol and Terfenol D, were appropriate thicknesses. Furthermore, 20 mm length and 4.8 mm width were detected as appropriate to continue electromagnetic simulations for all three materials. Electromagnetic simulations were performed by adding different types of super-strong neodymium permanent magnets and turns of the multilayer coil. Furthermore, resistance, inductance, and the number of turns of the coil were calculated for each simulation.

After evaluation, Metglas 2714A® Magnetic alloy and Terfenol D were deemed less suitable for this application because of their size and robustness. Optimized mechanical dimensions and electromagnetic parameters were suggested for ferromagnetic material to construct a bone conduction transducer prototype. It is suggested to use Galfenol alloy with 0.5 mm thickness, 20 mm length, and 4.8 mm for build a magnetostrictive transducer prototype for BC use by using a permanent neodymium magnet with 200-250 turns of the coil.

Keywords: Bone conduction implants, Galfenol, Resonance Frequency, Magnetostrictive transducer, Terfenol D, Metglas 2714A®.

Acknowledgments

I would like to thank my examiner Sabine Reinfeldt at Chalmers University of Technology, and my examiner Inci Cilesiz, at Istanbul Technical University, for your positive communication, guidance, and support throughout my thesis. They are a guiding light in this project. I would like to also thank my supervisor Dan Nyström, at Cochlear Bone Anchored Solutions AB, for answering all my questions and collaborating during my project. I would like to also thank my supervisor Dan Nyström, at Cochlear Bone Anchored Solutions AB, because he always gets enlightened and provided me to reach correct results during my study. He always replied patiently to all my questions. I would like to also thank Henrik Fyrlund and his colleagues at Cochlear Bone Anchored Solutions AB for allowing me to study this project. Last, I would like to thank Yalin Sonmez for helping with simulations and for his support at ANSYS® Electronics.

Contents

List of Figures

List of Tables

Abbreviations

a Acceleration
AC Air Conduction
B Magnetic flux density
BAHA Bone-anchored hearing aid
BC Bone Conduction
BCD Bone Conduction Device
BCHA Bone conduction hearing aids
BCI Bone conduction implants
BEST Balanced electromagnetic separation transducer
dB Decibel
F Force
GMM Giant Magnetostrictive Materials
K Spring constant
K33 Magnetomechanical Coupling Coefficient
MRI Magnetic resonance imaging
m Mass
mm Milimeter
N Newton
PZT Lead Zirconate Titanate
SPL Sound Pressure Level
SPAHA Subcutaneous piezoelectric attached hearing actuator
THD Total harmonic distortion
VRT Variable Reluctance transducer
WHO World Health Organization
ω Natural angular frequency
Φ Magnetic flux
μH Microhenry

Introduction

This chapter focused on the general outlines of the thesis. Some statistical information is included regards on the hearing losses. Besides, transducer types and main targets of the project were shortly mentioned. Limitations and motivation parts were explained in the thesis subject.

1. Introduction

Ear traumas and hearing losses are significant problems all over the world. The World Health Organization (WHO) predicts that nearly 2.5 billion people suffer from hearing loss, and at least 700 million will require hearing rehabilitation until 2050 [1]. These problems can have results that can affect people's lives. However, suffering patients can be helped with early diagnosis and treatment. Hearing devices and implantations are used in a therapeutic process. The primary purpose of rehabilitation is to enhance patients living conditions. Many facilities, research institutes, and companies enhance and review hearing implantations.

The main objective of the thesis is to test different transducer principles by design and physical prototype and by simulation. The aim is to study different designs and improve their cost, size, or performance. The literature review will tackle bone conduction technology and the magnetostrictive transducers working principle. The different applications and prototypes of bone conduction technology have been reviewed and improved for many years. It helps to support hundreds of thousands of people to hear every day. The motor for bone conduction is the transducer, transforming an electrical signal into mechanical vibrations. A transducer design can rely on piezo-driven, electromagnetic balanced and unbalanced, magnetostriction, and moving coil principle.

1.1 Background

Bone conduction has been used for many decades. However, it was matured at some research institutes and companies in the early days for enhancing hearing implantations. Cochlear Bone Anchored Solutions (Cochlear BAS) is one of the largest companies in bone conduction. This technology, which is based on the incoming soundwaves to transmit through skull bones of the cochlea today, helps hundreds of thousands of people to hear every day. It essentially works depending on a transducer principle that includes a motor. The motor used for bone conduction is the vibrator which transforms the electrical signals into mechanical vibrations. It can be designed to vary from piezo-driven, electromagnetic balanced and unbalanced, magnetostrictive material. The data of the planned vibrator may hold different measuring results depending on the properties of the material for which it is designed, and we desire to study how it can be more effective in terms of cost, size, and performance.

1.2 Aim

The main objective of this project is to find a new technique that has not been used in previous bone conduction devices, to provide maximum efficiency and sustainability in terms of size, cost, and performance. The essential material to design a new bone conduction transducer was investigated by literature studies, measurements, and discussions with supervisors at Cochlear BAS. This project focused on the possible utility of magnetostrictive material in bone conduction transducers. First, according to the literature studies and depending on the supervisor and examiner's comments, suitable materials are determined for comparison and testing by using simulation through ANSYS®. Then, according to the optimized simulation results, a magnetostrictive transducer design for bone conduction will be suggested to build a prototype that can be measured performance level in terms of efficiency force output, which may depend on the quality of the output signals.

1.3 Limitations

The ear functioning, hearing transmission pathways, and hearing conduction types will be mentioned without giving many theoretical details. Existing transducer technologies/principles used in bone conduction technologies will be discussed without including consumer electronics. It will be shortly mentioned the working principle of magnetostrictive transducers and mechanical fundamentals. The developed prototype will be compared with just the measuring results of other transducers. So, all transducers will not be compared with each other.

1.4 Motivation

This project will provide a different perspective on the development of bone conduction hearing devices. It will be investigated to find a possible magnetostrictive transducer replaced by the piezoelectric ceramic material, mainly used in the transducers used in the bone conduction (BC) hearing implants. Although the piezoelectric material has good properties for bone conduction transducers, it is pretty fragile [2]. This property makes it non-durable against impacts. In this project, the primary aim is to improve an alternative material with higher performance than piezo.

2

Background and Theory

This section focuses on theoretical knowledge about the content of the thesis. Firstly, human hearing physiology is explained. Then, bone conduction devices and transducers are discussed, respectively, with their used devices examples. Subsequently, the magnetostriction approach was detailed with properties and possible material examples. In the last part, the mechanical theory of transducers was focused.

2.1 Hearing physiology

The primary function of the human ear is to transmit the incoming sound signal to the hearing centers of the brain and convert it into neural signals. The transmitted sound signal follows the outer ear, middle ear, and inner ear structures in the ear and is transmitted to the hearing cortex in the brain. In addition, there is a neurophysiological function that starts in the outer ear and ends up in the auditory cortex in the brain for sensing hearing [3]. The primary structure of the human ear and its main parts is shown in Figure 2.1.

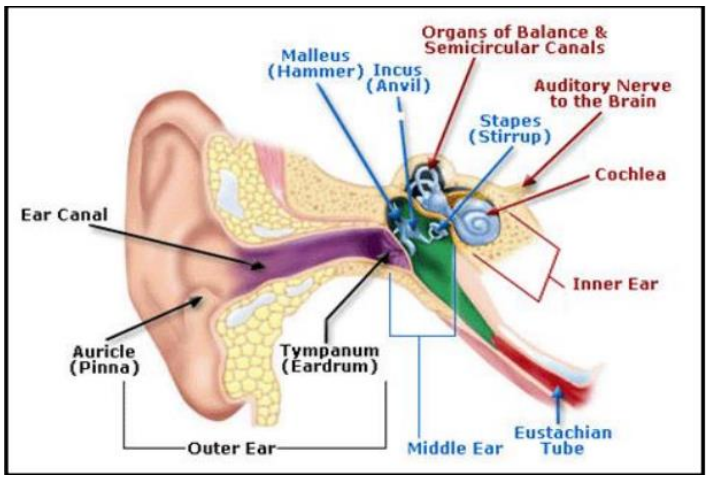

Figure 2.1: The human ear structure includes the outer ear, middle ear, and inner ear organs [4].

The incoming sound to the ear is transmitted to the auditory cortex in the brain through two different pathways. The combination of these two transmission pathways generates the hearing sensation. They are listed below:

- Air conduction (AC) hearing.
- Bone conduction (BC) hearing.

2.1.1 Air conduction hearing

The transmitted sound signal is processed in the relevant cortex of the brain after the sound transmitted to the ear via (AC) or (BC) and creates the hearing sensation. The AC follows the pathway below until the sound signal respectively reaches the cochlea of the ear:

- The Ear Canal, Eardrum, and Middle Ear Ossicles.

The outer ear comprises the ear canal with an S-shaped path and pinna, the first connection place of sound energy that incomes from outside. It amplifies the sound pressure, which has not arrived yet at the tympanic membrane through the mechanism referred to as the ear canal resonance with about 15-20 dB in the frequency range of 1.5 to 7 kHZ [5].
The middle ear has a mission that is an impedance transformer. This operation enhances incoming sound waves to the inner ear. Without this function, the transmitted sound waves would be between 25 and 30 dB lower [6]. The middle ear operates as a mechanical amplifier and performs the amplification based on three following principles. The first mechanism that provides the most considerable amplification is the size difference between the oval window and the tympanic membrane. Secondly, the amplification principle is regarding the shape of the curved tympanic membrane. The third structure is the lever advantage based on the ossicular chain [7]. The sound waves are transformed into fluid vibrations that cause hearing in the inner ear. The inner ear is a canal that involves the cochlear structure, which is filled with fluid and has spiral-shaped. The movement of the stapes footplate in the oval window causes the beginning of sound processing in the inner ear. The mechanical pressure change caused by the movement transform to pressure variations in liquid. It is shown in Figure 2.2 that the Basilar membrane and Reissner's membrane provide the separation of three divided layers of the cochlea [8]. The vibrations are transmitted to the oval window structure, which vibrates the inner ear.

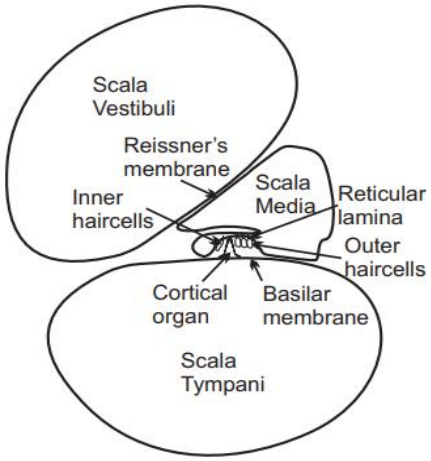

Figure 2.2: The cochlea structure includes one outer and inner layer[8].

The fluid in the cochlea begins to move as the mechanical vibrations are transmitted to the oval window. The relevant signals simultaneously begin to excite and vibrate the basilar membrane depending on their frequency values. The vibration level is based on frequency values in different parts of the cochlea. Therefore, the Cilia found in hair cells start to move based on the stimulated basilar membrane.

The inner section of hair cells generates some nerve impulses sourced from mechanical vibrations. Then, these impulses are transmitted to the auditory cortex of the brain.

2.1.2 Bone conduction hearing

Bone conduction (BC) is presently useful for all people who suffer from hearing traumas. This theory, based on vibrating things that can transmit sound, was first introduced by Girolamo Cardano in the 1500s [9]. In this principle, the sound wave is transmitted directly to the cochlea, bypassing the ear's outer and middle ear parts. Instead, this transmission occurs via mechanical vibrations from skull bones to the cochlea. This process is ended up stimulating the cochlear nerve [10]. Bone conduction and air conduction transmission pathways are shown in Figure 2.3.

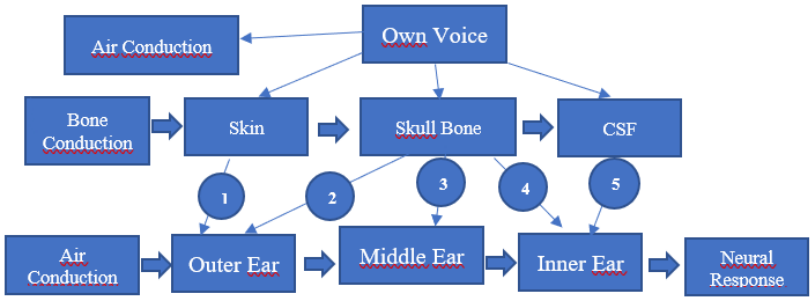

Figure 2.3: The pathway of hearing function is inspired by [10]. 1. Soft Tissue Vibration. 2. Bone Vibration. 3. Inertial Forces. 4. Inertial Forces. 5. Sound Pressure.

The results of these parameters may vary depending on the active frequency values. According to this statement, the inertia of the cochlear fluid is the most remarkable factor lower than 4kHz, and it will lose efficiency as long as it increases of frequency value [11]. Moreover, the middle ear ossicle inertia contributing factor affects the BC in the frequency values between 1.5 and 3.1 kHz [12].

2.1.3 Hearing Losses

Hearing impairments can be shortly described as the loss of hearing abilities. It can be permanent or temporary, depending on the level of loss. They could be originated from environmental or biological factors. They can be classified as follows :

- Conductive loss.
- Sensorineural loss.
- Mixed hearing loss

Sound waves are not adequately transmitted to the cochlea via the outer and middle ear with conductive loss. A bone conduction hearing aid is an excellent rehabilitation option for this type of loss.

2.2 Bone conduction devices

Bone conduction devices can be reviewed in two main parts and are classified [13].

- Skin drive devices.
- Direct drive devices.

The main categorization of bone conduction devices is demonstrated in Figure 2.4, and a discussion of each type will follow in this sub-chapter.

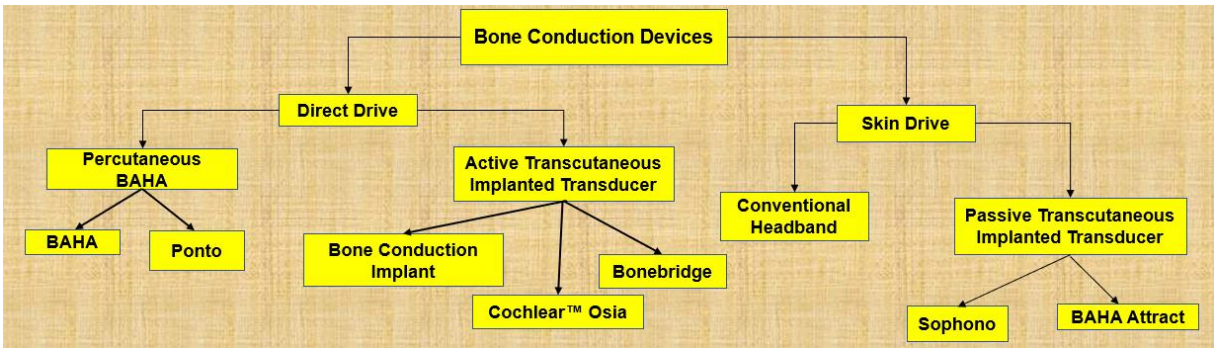

Figure 2.4: The categorization scheme of bone-conduction devices is shown by modifying to exclude devices currently not on the market, inspired by [13].

2.2.1 Conventional Bone Conduction hearing devices

At the beginning of the 20th century, conventional BC hearing devices matured with a sound processor attached to spectacles, steel spring headbands, or soft headbands[9]. They are positioned outside the skin and are pretty easy to use. They do not require any surgical process and have a bone conduction transducer, amplifier, microphone, and an audio processor. Mechanical vibrations are transmitted to the skull from the skin after an external transducer produces the stimulating vibrations. A static force of 2N is pressed towards the skin on the skull since it is needed to transmit vibrations properly [14]. Moreover, the conventional bone conduction device example is shown in Figure 2.5. They may cause some skin problems depending on the long-term use. Skin problems may give rise to blood circulation problems and eventually necrosis. There are also some efficiency disadvantages of these conventional BC devices. There is vibration damping from the subcutaneous tissue [14]. This decreases sound quality, which is insufficient against too high noise environment. Moreover, it can cause discomfort caused by applying static force, which causes pressure on the skin. This effect may give rise to getting pain.

Figure 2.5: A conventional bone conduction device [13].

2.2.2 Bone anchored hearing aid

Percutaneous bone-anchored hearing aid (BAHA) was developed between Chalmers University of Technology and Sahlgrenska University Hospital in the 1970 [15].

BAHAs were intended to be produced as an alternative to conventional hearing devices. The main operating principle of BAHA is the direct transmission of vibrations to the skull bone for efficient transmission of high-frequency sound. At this point, the soft tissue is bypassed during transmission, unlike conventional hearing aids. So, the skull bone is directly stimulated. They include two main components: an electromagnetic motor that enables inertial mass to provide force for the abutment and an abutment connected with a screw (titanium fixture) to the mastoid part of the skull bone. The main electronic components of BAHA are shown in Figure 2.6.

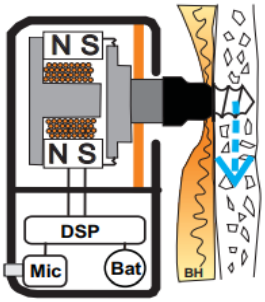

Figure 2.6: The main components are in the BAHA, a microphone, battery, and power amplifier[16].

2.2.3 Transcutaneous BC Hearing Aids

Conventional and percutaneous BC hearing aids are still used to rehabilitate hearing traumas; however, transcutaneous devices that significantly keep intact skin have been developed. They can be categorized as passive and active devices[13]. The passive transcutaneous devices are pretty similar to conventional hearing aids. Its only and most significant difference is using a permanent magnet to remain more stable of devices attached under the skin instead of a steel spring or headband[13]. The working principle of the passive transcutaneous devices is shown in Figure 2.7.

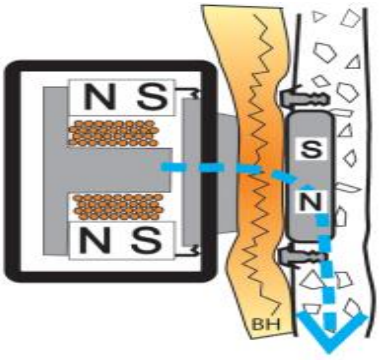

Figure 2.7: The structural design of a passive transcutaneous hearing device uses an implanted magnet instead of a headband[16].

The second class is the active transcutaneous devices that transducer is directly attached to the skull bone under the skin. A prototype of the device example is shown in Figure 2.8. A direct connection facilitates bone conduction. It keeps the skin intact, and there is no permanent penetration. They include loss suffering from the acoustic feedback since the microphone and transducer are separately located. It has been detected the less transmission loss and has better high-frequency gain than the passive devices. They involve implanted and external magnets. Bone conduction implants can be an excellent example of active transcutaneous aids. They will be reviewed in more detail in the next section.

Figure 2.8: An example image of active transcutaneous BCD includes implantation and external section[14].

2.2.4 Active transcutaneous bone conduction devices

According to the studies, active transcutaneous BCDs ensure a suitable rehabilitation solution for hearing indicated losses [17]. They are preferred as an alternative to the BAHA system since they leave the skin intact by using the wireless solution to remove permanent skin penetration and provide direct stimulation in the skull bone. There are several devices that have the working principle of this type and the next chapter focuses on the Bone Conduction Implant (BCI).

2.2.4.1 Bone Conduction Implant

The BCI comprises the external and implanted unit. The external unit is covered in a plastic housing and comprises a battery, an external magnet, an audio processor containing a microphone, an analog and digital signal processor, and a power amplifier.

The implanted unit that can be implanted into the skull includes the receiving coil, an internal magnet, demodulator, and BC transducer that does not use a screw for attachment. This transducer contacts the mastoid bone using a flat surface[14].

Moreover, the components of the implanted unit are sealed in a titanium housing, and it is covered with compatible material like silicone, except for the part in contact with the mastoid for osseointegration. We can see components of the implanted and external unit in Figure 2.9.

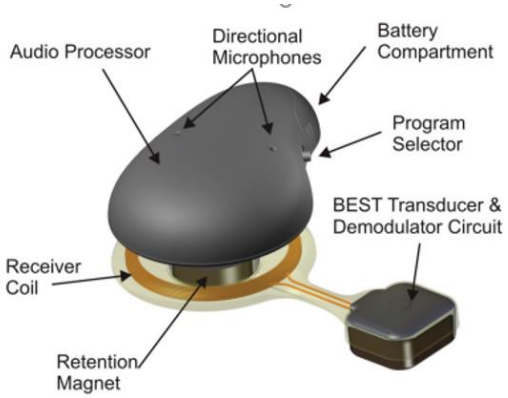

Figure 2.9: The components of an implanted and external unit of BCI [18].

The transmission between implanted and external units of BCI is ensured by inductive linking activated by a specific integrated circuit on the external unit of BCI. Besides, it delivers the transmission of signal and energy for this inductive linking by the power amplifier located on the external unit [19]. The transmission between implanted and external units of BCI is ensured by inductive linking activated by a specific integrated circuit on the external unit of BCI. Besides, it delivers the transmission of signal and energy for this inductive linking by the power amplifier located on the external unit[19]. Digital filters process incoming sound from outside after it is converted into an electrical signal by a microphone found in an external unit. Then, amplitude modulated via an inductive link for this signal is done. Finally, this processed signal will be demodulated before being transmitted to the bone conduction transducer, which transmits vibrations to the skull bone [19]. It is illustrated in the working principle and transmission way of vibrations in Figure 2.10.

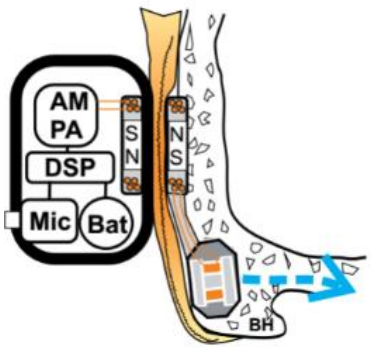

Figure 2.10: BCI's components are amplitude modulation (AM), power amplifier (PA), microphone (Mic), battery (Bat), and digital signal processor(DSP) [16].

It is transmitted the signal to the BC transducer that operates the BEST principle after the demodulation process of the processed signal is finalized. Next, the acquired vibrations are transmitted via skull bones to the cochlea by the transducer. Then, the fluids of the cochlea are stimulated. There is a crucial point here regarding the location of the transducer. It was determined to increase the sensitivity of bone-conducted sound if the BC transducer is implanted to be placed closer to the skull bone [20]. In the BCI principle, BCI's transmitted BC sound sensitivity is higher than BAHA since the bone conduction transducer is closer to BAHA[19]. Moreover, the implanted place of the bone-conduction transducer can be called the excitation point. According to the study, it was detected that there is a signal attenuation that causes a power loss of around 10-15 dB sourced from the use of inductive coupling in BCI; however, it seemed that this issue could be tolerated by placing the excitation point is closer the cochlea[20].

2.3 Bone conduction transducers

Air conduction (AC) and bone conduction (BC) hearing threshold tests are applied to patients who have been suspected of suffering from hearing traumas. The obtained difference between thresholds in AC and BC gives a result regarding the conductive hearing loss. They are analyzed together with the data of AC thresholds measuring for sufficient alternative rehabilitation after the BC hearing thresholds are tested using a bone conduction vibrator. We will focus on the BC vibrators used in bone conduction hearing aids below.

2.3.1 Conventional electromagnetic transducer

Conventional electromagnetic transducers can be called unbalanced transducers as well. It involves airgap, soft iron, magnet, coil, and spring. The structural view of this transducer is illustrated in Figure 2.11.

There are different procedures for acquiring vibrations. First of all, the mechanical force and magnetic force must balance. The direction of the current flowing through a coil in the closed loop will affect the level of the magnetic force, and magnetic force can increase or decrease depending on the direction of the current flowing.

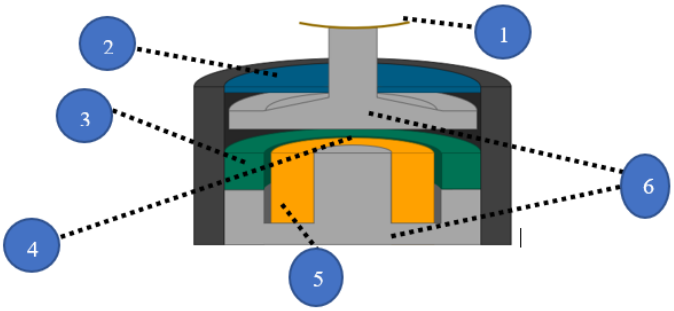

Figure 2.11: The structural view of the conventional transducer is inspired by [21] : 1. Coupling 2. Spring 3. Magnet. 4. Air-gap. 5. Coil. 6. Soft Iron.

2.3.2 Variable reluctance transducer

A BC transducer activates a time-varying current, and the obtained vibrations are transmitted as electromechanical. Current follows the pathway of coils on the transducer for achieving a time-varying flux. The combination of time-varying flux and static magnetic flux creates the total magnetic flux in the transducer. There is a nonlinear relation between the total magnetic flux and the total vibration force of the transducer. This effect causes harmonic distortion at low frequencies. Besides, nonlinearity can be negligible for small values of total magnetic flux. However, it will not be valid for high values of that. This situation causes an inconsistency in bone conduction processes, so nonlinearity should be eliminated as much as possible. It can be used as a permanent magnet with higher static force and magnetic flux to minimize this effect, but it causes a higher resonance frequency. However, a low resonance frequency is needed in the bone conduction processes. The structure of a variable reluctance transducer (VRT) is shown in Figure 2.12.

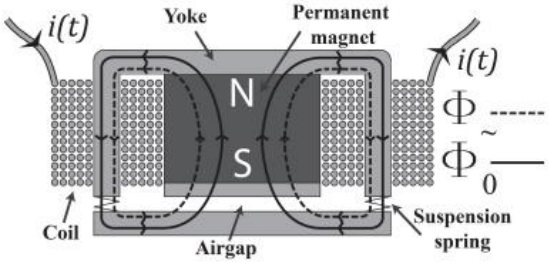

Figure 2.12: The structural view of VRT in Radio-ear B71 BC vibrator [22].

2.3.3 Balanced electromagnetic separation transducer

A balanced electromagnetic separation transducer (BEST) was matured by Hakansson(2003)for tolerating low-frequency problems in variable reluctance transducers [23]. It was designed that is to intended to use in bone conduction vibrators. The primary purpose of BEST is to remove the nonlinearity effect. The harmonic distortion decreases by the minimized nonlinearity. Moreover, it includes more inner and outer air gaps balanced as static, compared with variable reluctance transducers. The time-varying flux increases dynamic force by flowing closed-loop on the inner and outer air gaps. Also, there are four permanent magnets in these airgaps, and they ensure to boost of the static magnetic flux.

Therefore, this more balanced structure cause to cancellation of static and nonlinear effects and offers a more effective, more minor, and simple design for implantation studies. In addition, it increases the maximum hearing levels. A circuit design of BEST which includes air gaps and magnets is illustrated in Figure 2.13.

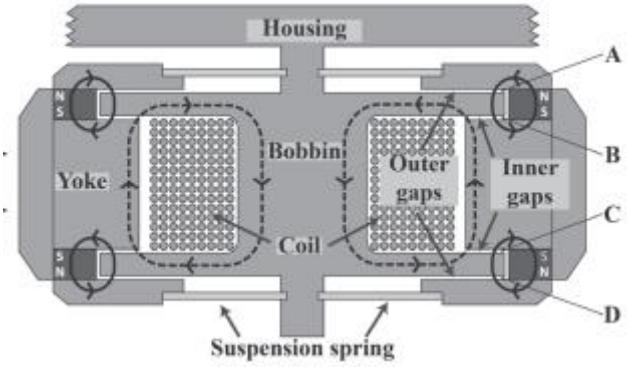

Figure 2.13: The design view of BEST which includes air gaps and magnets [22].

2.3.4 Piezoelectric transducers

This device's operating principle is to create an electrical current by applying force [24]. It was determined that some materials that hold the piezoelectricity effect could generate strain more than ten times more than traditional materials [25]. The piezoelectricity effect can be called the ability to create vibrations to respond to the incoming electric signals from the signal processor. An unimorph structure of the piezo materials enables it to act as a mechanical transformer that conducts high-amplitude vibratory motion and in materials. These materials have started to be used in bone conduction vibrators in recent years. In the 2010s, a new subcutaneous piezoelectric attached hearing actuator (SPAHA) was presented, and Unlike a BAHA transducer, this device generates a localized bending moment [25]. SPAHA includes a transducer-based on a uni-morph piezoelectric material on Lead Magnesium Niobate-Lead Titanate (PMN-PT) piezo single crystal. This crystal has a powerful potential for hearing implantations [26]. An elastic bending principle stimulates the cochlea instead of applying point a force. Moreover, it does not require an inertial mass. The structure of the unimorph material during bending is shown in Figure 2.14.

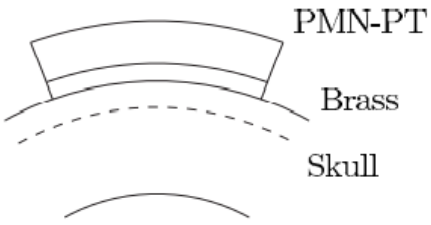

Figure 2.14: The structural view of SPAHA during bending [25].

It was noticed that the piezoelectricity-based transducers show better results in mixed hearing impairments [27] and they achieve the required high-frequency output. In addition, it has a lower cost and eases manufacturing. In another study, Lead Zirconate Titanate (PZT) was used in the transducer as a piezo material [26].

In that, voltage displacement occurred as linear. The linearity facilitates signal processing operations in implantation applications.

According to the working principle of the piezoelectricity actuators, the layers of piezo material start to bend firstly, and this operation causes increases in counterweight. That gives rise to generating vibrations. Then, the vibrational energy that appears is transmitted to the mastoid. In recent times, The Cochlear™ Osia® 2 System (Cochlear Bone Anchored Solutions, Sweden) was presented as a new active bone conduction transcutaneous hearing implant system that includes a transducer-based on piezoelectricity. A digital piezoelectric stimulation principle to transmit sound to the cochlea was first utilized instead of electromagnetic stimulation in the Osia implantation systems by Cochlear BAS. This principle provides to enhances high-frequency gain. Some tests can tolerate a hearing loss of up to 55 dB, and compared with Baha®5, Cochlear™ Osia® 2 System offers a higher functional gain in higher frequencies (5–7 kHz [28]. An additional gain of 19.3 dB at 6000 Hz was detected compared with Baha® Attract in the Osia system. This gain may be sourced from a piezoelectricity actuator[28]. An additional gain of 19.3 dB at 6000 Hz was detected compared with Baha® Attract in the Osia system. This gain may be sourced from a piezoelectricity actuator [28] and primary from using direct stimulation in the bone. This active osseointegrated implant structure provides high power output, and the patients are satisfied with using those. The components of Osia™ are shown in Figure 2.15 and Figure 2.16.

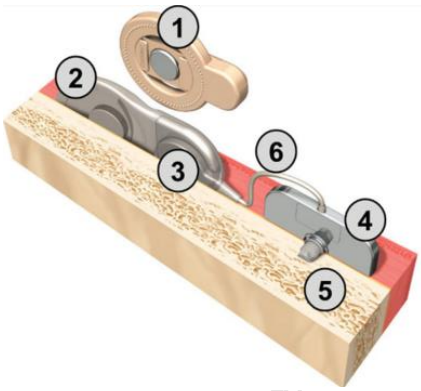

Figure 2.15: The Schematic illustration of the Osia™ *[28]:* 1. External processor 2. Receiver 3. Stimulator. 4. Piezoelectricity actuator. 5. Titanium screw. 6. Coil.

Figure 2.16: Cochlear™ Osia® System implants[29].

2.3.5 Ranking and classifying bone conduction transducers

Previous chapters discussed conventional electromagnetic transducer, variable reluctance transducers, a balanced electromagnetic transducer, and piezoelectric transducers. This section will focus on ranking and classifying them in different parameters.

The B71 BC vibrators, based on the variable reluctance transducer (VRT), were frequently used in BC audiometry. However, they have a large structure and hold problems such as non-efficiency output and nonlinear distortion at low frequency regarding efficiency. In order to eliminate significant drawbacks of efficiency problems of B71 vibrators, a new transducer was developed called Balanced Electromagnetic Separation Transducer (BEST) by Bo Håkansson(2003) [23]. In comparison with VRT, this new transducer principle had some advantages. It had a smaller structure than VRT and was suitable for hearing implants. It was detected that the total harmonic distortion level in BEST was smaller than in VRT at low frequencies. Also, the number of balanced and static air gaps in BEST was more than in VRT. The investigations determined that it has a more efficient output, smaller structure, and easier fabrication of BEST principle than VRT.

Furthermore, it was obtained that the BEST principle offers boosted sensitivity and enhanced efficiency depending on higher input impedance, measured thresholds of bone conduction at 250 and 500 Hz with better accuracy, and has a lower counterweight mass [22]. These views show that the BEST principle offers more effective output than conventional bone transducers.

Therefore, the Radioear B81 BC vibrator that operates based on the BEST principle was developed instead of the B71 [30].

The next time, a new transducer has developed based on piezoelectricity instead of electromagnetic material. The piezoelectric material in this transducer can produce strain more than approximately ten times than the used materials in conventional bone conduction transducers [25]. In addition, it was determined that piezoelectricity-based transducers have lower total harmonic distortion (THD) levels than previous bone conduction transducers[26]. THD level is directly related to the nonlinear distortion. In that case, the distortion level is reduced, relying on the transducer's low THD level.

Furthermore, it was detected that there is lower power consumption in piezoelectricity transducers than in electromagnetic bone conduction transducers. Also, it can be said as advantageous in terms of commercial due to its lower cost and easier manufacturing. Furthermore, according to some benchmark tests, it was shown that the piezoelectricity vibrator offered wider bandwidth, shorter release time, and faster response and was detected to achieve high compatibility with the external magnetic field. Moreover, it holds a better quality of sound transmission than the other transducer principles [31].

2.4 Magnetostriction

Magnetostriction allows for the expansion or contraction of ferromagnetic materials. This property appears when magnetic materials hold a response in a magnetic field. In addition, the

magnetostrictive effect provides to convert between energy forms. It can be given an example of electromagnetic energy into mechanical energy.

The magnetostriction effect was firstly detected and measured on iron material by James Prescott Joule[32]. So, it can be called as Joule Effect. This effect can be described as the change in length of a ferromagnetic material exposed to the magnetic field. So, it achieves elongation or shortening of ferromagnetic material for a direct effect. Also, the magnetostriction effect can happen during realignment that causes extension or contraction of the ferromagnetic material. Therefore, the Joule effect is most used in magnetostriction applications.

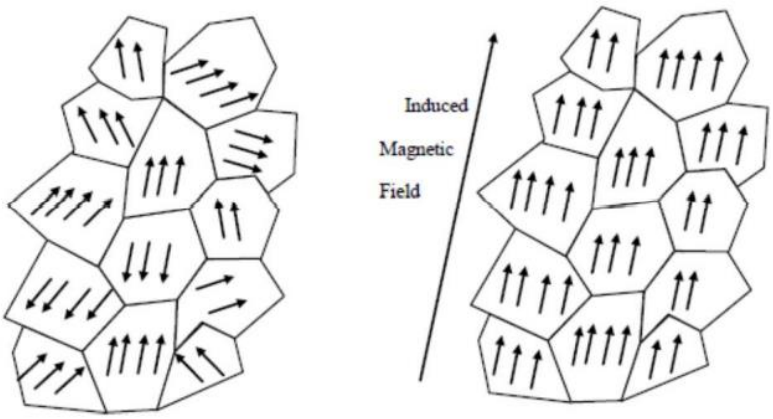

Figure 2.20: The realignment principle in the magnetic domain[33].

Following, the Villari effect that can be called the converse joule effect was discovered by E. Villari [34]. According to this opposite effect, the stress applied to the ferromagnetic material causes to create a magnetic field over the same material. According to another effect that Gustav Wiedemann approached, the twisting in the ferromagnetic material will occur when subjected to a magnetic field that is circular or longitudinal[35]. This approach was called the Wiedemann Effect. Next, it occurred a Matteucci effect an opposite the Villari effect.

2.4.1 Magnetostrictive Properties

There are some significant points regarding the magnetostrictive concept. These are explained as follows.

- **Ferromagnetism**

Ferromagnetism is the electrically uncharged materials attracted to the other materials. Ferromagnetic materials can be easily magnetized in powerful magnetic fields. Examples are iron, nickel, and other alloys. Some specific criterias are used to evaluate the efficiency performance of the magnetostrictive material. Significantly, they must be considered when the new application is designed. These criteria can be sorted as follows [36] :

- **Magnetostrictive Coefficient**

Magnetostriction coefficient provides to be correctly calculated of the magnetostriction. The change in length is divided by the original length as the magnetization rises from zero to saturation.

- **Saturation Magnetostrictive Coefficient**

This effect corresponds to the moment that the material obtained maximum alignment. Thus, it seems the maximum magnetic moment can be obtained.

- **Magnetomechanical Coupling Coefficient (K33)**

This parameter that depends on the boundary condition of induction of magnetic field is directly related to the ability of the material to convert magnetic energy into mechanical energy and can be occurred vice versa. It is named K33, and this numerical value must be between 0 and 1. Also, it is remarked as being a dimensionless parameter.

- **Permeability**

Magnetic permeability explains the response of magnetic material that is applied in the magnetic field. Magnetic materials can be classified based on their magnetic permeability properties are are non-permeable, diamagnetic, paramagnetic, and ferromagnetic[37]

2.4.2 Magnetostrictive Materials

This section will briefly mention the properties of the possible magnetostrictive materials utilized for a new bone conduction transducer.

Giant Magnetostrictive Materials (GMM)

Terfenol D and Galfenol alloys will be reviewed in this group. It was noticed that they have a high level applicable for designing a new transducer.

Terfenol D

Terfenol D alloy, comprised of Iron, Terbium, and Dysprosium, has pretty high-level magnetostrictive abilities, and it is used chiefly for its magnetostrictive properties. The shape of this alloy will be changed when exposed to the magnetic field. Moreover, it can create higher internal strain in the magnetic field than conventional magnetostrictive alloys[37]. It means actuators that consist of Terfenol D are more powerful and have more significant displacement[38]. It can convert electrical power into mechanical motion and vice versa. This ferromagnetic material can be easily adapted to outside conditions. The permanent magnet and rod that includes a coil are used[33]. On the other hand, the response time is rapid for this alloy. This property is pretty significant for high-force vibrators [39]. The advantages characteristics of this material are as follows:

- High Compressive Strength
- High Force
- Wide Bandwidth
- High Reliability/Unlimited Cycle Life
- Wide Temperature Range
- Fast Response

There are some disadvantages properties of this alloy as well. Compared with piezoelectricity, it has a bigger size and a more complex structure [39]. Furthermore, it has a brittleness structure against the impact forces [40].

Galfenol

The Lead Zirconate Titanate (PZT) has a pretty brittle structure and is weak against impact forces. Also, the Terfenol-D alloy has trouble regarding processing parts, and it requires a complex magnetic circuit with a winding coil which includes many turns because of low permeability. Therefore, a new alloy called Galfenol, which is comprised of Iron and Gallium, was developed to solve these problems with previously mentioned alloys [41][42]. This new alloy had better mechanical properties than Terfenol D and PZT. It has high stability against external forces, and this property can be successfully performed with some forces without any problem. These forces can be sorted as impact, tensile, and bending[43].

Metals, Alloys, and Derivatives

Some other alloys have magnetostrictive abilities except for the ones mentioned above. The standard alloys comprised of nickel, cobalt, and iron have a low magnetostrictive ability; however, the other magnetostrictive alloys are based on Terbium, Dysprosium, and Iron Gallium can have better magnetostrictive properties[44]. Some alternatives were tried to improve materials with low magnetostriction ability, and alloys with amorph structure were produced [33]. These developed alloys offer extremely high permeability and low power loss.

2.5 Transducers

Transducers are utilized to transform the electrical signal from another form of energy. They are primarily used to convert to the electrical signal from mechanical energy. Besides, their operation principle is almost the same as a spring-mass system[45]. Transducers have two main parts: a motor unit and a mechanical system. The motor unit can be comprised of electromagnetic or magnetostrictive materials. The mechanical system of the transducer is explained by the mass spring system. Transducers are needed in bone conduction hearing aids. They ensure to transmit the obtained vibrations to the related parts such as abutment, skull bone. The vibrations are transmitted to the attached implant after the incoming soundwaves are converted to the vibrations by a related party in the external unit. Implants vibrate to the bone around the cochlea. Hence, bone conduction hearing devices that include a transducer can be evaluated as a spring force system involving a motor unit[45]. The operation principles of magnetoelastic transducers will be mentioned. In addition, an example of the magnetoelastic unit of a transducer is shown in Figure 2.21.

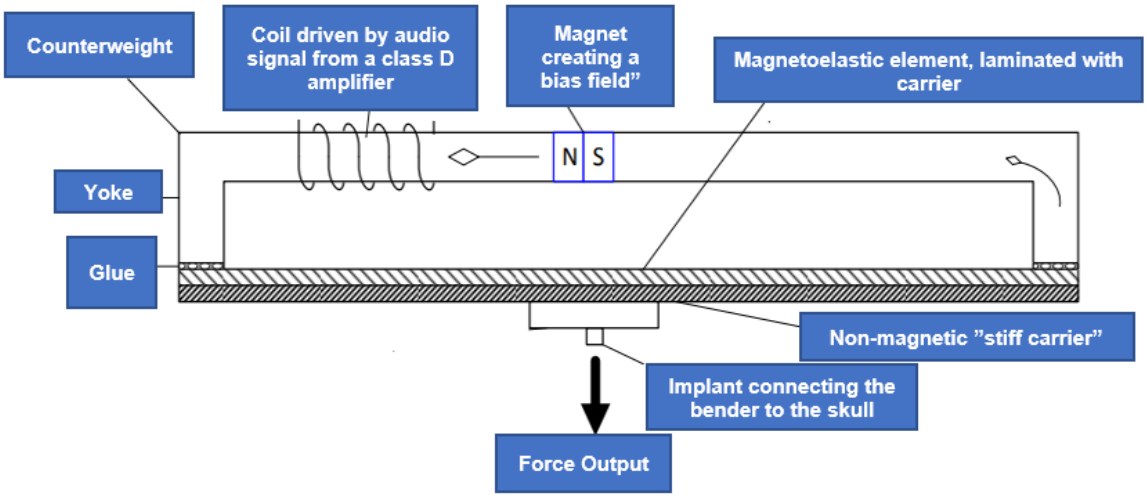

Figure 2.21: A basic model of magnetoelastic transducer[46].

2.5.1 The working principle of a magnetoelastic transducer

In magnetoelastic transducers, the dimensions of magnetostrictive material are altered when it is magnetized. An oblong shape of material will hold the most extended length if magnetization occurs in the axial direction.

It forms a bender by laminating magnetostrictive elements onto the non-magnetic material. Then, the bending structure is attached to the yoke with glue or similar material. Moreover, it should be paid attention that the tape is to be attached to avoid the yoke's deformation due to the bender's movement and allows lateral movement.

Furthermore, there is a magnet that is attached to the yoke. It is used to generate a magnetic flux that biases the magnetization of the magnetostrictive material.
A coil would modulate this magnetic flux. A class D amplifier drives this coil. The modulation process should be minor from the bias field. Also, it would get advantageous at the initial position being of the bender when the static bias field is applied.

The lamination process of the magnetoelastic element to the non-magnetostrictive material has to be ensured either with the materials being in a curved shape or by a strain applied to the carrier.

The variations of magnetization of the magnetostrictive material create a bending deformation of the bender. The mass of the yoke in the system will amplify the force output and appeared movement. At this point, it can be generated a combination with the mass of the yoke by adding a weight mounted in the center of the bender. In order to deliver the force output, the center of the bender is attached to the skull bone of the patient.

2.5.2 Mechanics

There is a relationship between mechanical vibrations, mechanical operations of transducers, and the spring-mass system. According to this system, there is an amount of mass going back and forth on a spring. This motion of the mass is called harmonic motion. It is assumed that there is a mass sitting on some frictionless surface at the beginning.

This mass is attached to the spring and, in the beginning, at rest. It would be kept in an equilibrium position if it could not have touched anything. However, it can move away from the equilibrium location if it is touched. At this point, the spring would want to return to the initial point, but it can not do it directly, so it moves back and forth. This system should analyze the forces if it wants to represent a numerical model. Then, Newton's second law can be utilized, explaining that the total force **F** is equal to the mass **m**, times the acceleration, **a.** We can see that in equation 2.1.

$$F = ma \tag{2.1}$$

The acceleration should be written, **a**, as the second derivative of the displacement, **x**.

$$F = mx'' \tag{2.2}$$

The relevant force for the frictionless surface in the above equation at the beginning is explained by Hooke's law which presents the force of the spring acting on the mass. According to Hooke's law, minus **k** is just spring constant times **x,** which is the displacement from equilibrium. The spring constant,**k**, depends on the properties of the spring. For example, it may be a larger value if there is a thick coil.

$$F = -kx \tag{2.3}$$

In this system, it is assumed that there is a vertical line where the spring would like to be at rest. If it is moved from rest, a displacement from equal to zero would be obtained, being that equilibrium position that's the x in Hooke's law. A differential equation for the system is obtained in equation 2.4. We will have a sinusoidal function as the solution. See equation 2.5 after it is solved of equation 2.4.

$$mx'' + kx = 0 \tag{2.4}$$

$$x(t) = A\sin(\sqrt{(k/m)}*t+\theta) \tag{2.5}$$

Time is **t**, the phase angle is the **θ,** and the vibration amplitude is **A**. It will obtain results about **A** and **θ** by considering the initial position and velocity of the mass. Hence, the material's natural frequency can be calculated using a mass-spring model.

$$\sqrt{(k/m} = \omega \tag{2.6}$$

$$x(t) = A\sin(\omega t+\theta) \tag{2.7}$$

This **ω** value is called natural angular frequency because the sine and cosine oscillating terms oscillate faster if it gets larger values of **ω**.

A system's natural frequency can be described as the frequency at which it will oscillate naturally when in free vibration. Hence, it is understood to vibrate at a high amplitude at the natural frequencies of material. Natural frequencies may vary depending on the material's stiffness or mass. Besides, there is no applying an external force.

2.5.3 Electromagnetism

Electromagnetism is one of the four fundamental forces of nature. All matter has an electric charge which can be positive, negative, or zero. Electromagnetism is the physical force that causes the interaction between electrically charged particles. Magnetic force is directly related to the motion of charges in a magnetic field. The charge in motion is exposed to the magnetic force, Fm. This force can be explained in see equation 2.8. In that, v is velocity, q is a charge, and B is the magnetic field strength.

$$\boldsymbol{Fm = qv \times B} \tag{2.8}$$

It should be looked at in Lorentz's Magnetic Force law to calculate the electromagnetic force. Then, according to the equation, the electric field of strength should be added to the magnetic force formulation, and the equation is shown in 2.9.

$$\boldsymbol{F = q(E + v \times B)} \tag{2.9}$$

Magnetic flux will be obtained by integrating magnetic field strength on the surface, see equation 1.1.

$$\boldsymbol{\Phi = \int_S B.ds} \tag{2.10}$$

The electromagnetic force will be the driving force in the transducer system. The equation below shows that this force can be expressed in magnetic flux Φ [45].

$$\boldsymbol{F \propto \Phi^2_{tot}} \tag{2.11}$$

Total magnetic flux, Φ_{tot}, is equal to the sum of dynamic magnetic flux, Φ_D, generated by an exciting coil, and static magnetic flux, Φ_s, created by a permanent magnet. This mathematical formulation is shown in equation A.A.

$$\boldsymbol{\Phi_{tot} = \Phi_s + \Phi_D} \tag{2.12}$$

3

Materials and Methods

This section focuses on the different analyses with simulations of a magnetostrictive transducer for bone conduction use. According to the literature review, material selections used in simulations were listed in tables. They were performed through mechanical and electromagnetic simulations in ANSYS® Mechanical and ANSYS® Electronics. According to the data of mechanical simulations, the sizes of magnetostrictive material of the model were optimized, and were performed simulations with different parameters to measure the average magnetic field density of the bender in the transducer.

A working flow chart of simulations in ANSYS is shown in Figure 3.1.

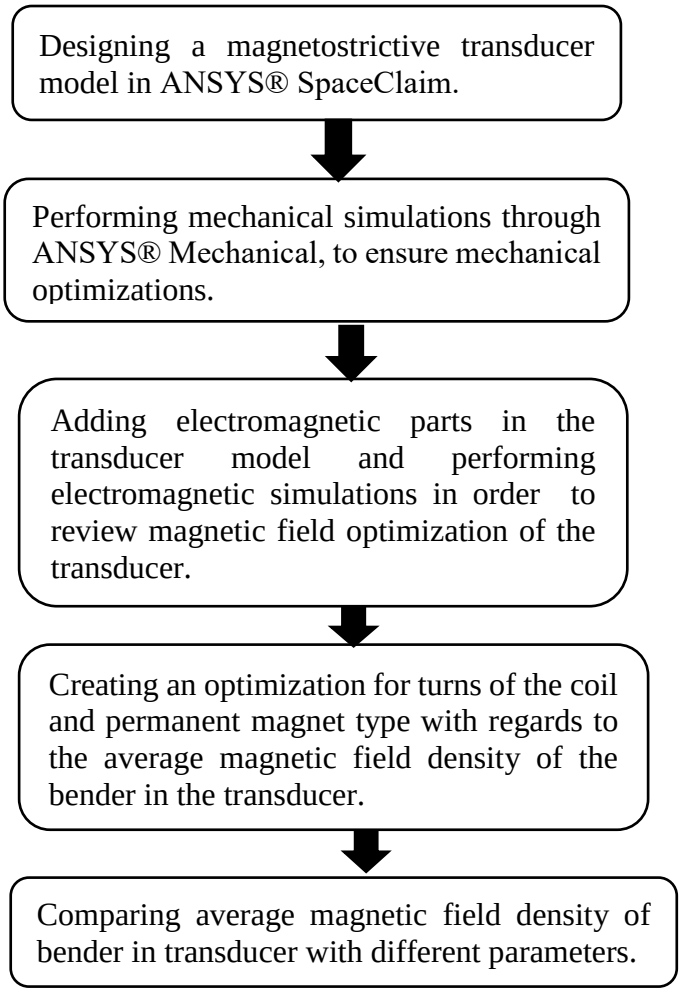

Figure 3.1: The flow chart of simulations.

3.1 Model Design

A magnetostrictive transducer consists of both electromagnetic and mechanical parts. A bone conduction transducer model with mechanical parts was designed through ANSYS® Mechanical. This design included a counterweight, a magnetoelastic element, non-magnetostrictive material, and a connector. It forms a bender by laminating magnetostrictive elements onto the non-magnetostrictive material. Then, the bending structure is attached to the counterweight with glue or similar material. This model is shown in Figure 3.2.

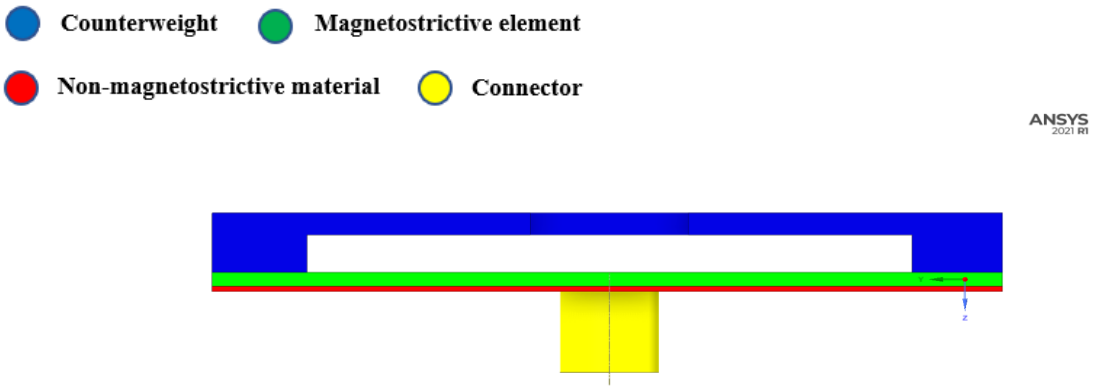

Figure 3.2: Mechanical model was designed through ANSYS® Mechanical.

Another part was about adding electromagnetic parts to the transducer, and included parts were a coil, a permanent magnet, and a core. The permanent magnet, which creates a static magnetic field, is integrated into the counterweight. The coil generates dynamic magnetic flux and is attached to the counterweight. Furthermore, the counterweight was used as a core for the coil in the electromagnetic field.

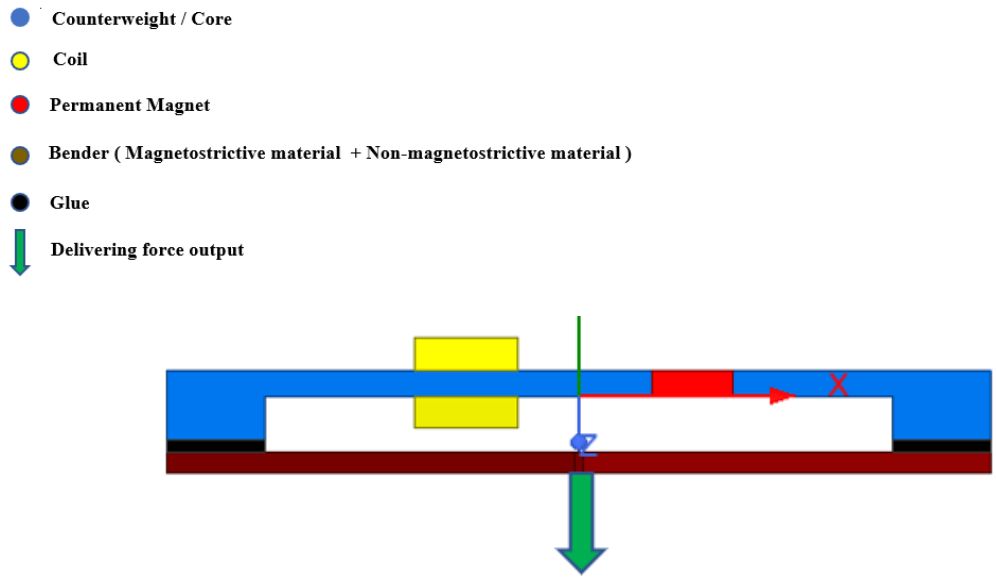

Figure 2.17: 2D representation of magnetostrictive bone conduction transducer through ANSYS Electronics.

3.2 Material Selection

The different materials were selected for the different parts of the model for simulations. Silicon Core Iron was chosen instead of Tungsten which is primarily used for conventional electromagnetic transducers, as a counterweight used as a core for the coil and the electromagnetic field in this model. The electrical and permeability properties of materials played a crucial role in selecting the counterweight part.

Neodymium super-strong permanent magnets were preferred for simulations because they will provide better magnetization. Furthermore, copper was selected for the coil. The material selections for simulations are listed in table 3.1.

According to the literature review, three possible magnetostrictive materials have been chosen in order to test, and they can be sorted as follows :

- Terfenol D / Galfenol (Iron-Gallium) / Metglas 2714A ® (Cobalt-based alloy)

Material Selection	Counterweight / Core	Coil	Magnetostrictive Material	Non-magnetostrictive Material	Tape	Permanent Magnet
Part of the transducer model	Silicon Core Iron Alloy	Copper	Terfenol D / Galfenol / Metglas 2714A	Aliminium	Rubber, TPC (Shore D70)	N48 / N50 / N52

Table 3.1: Material selection for the simulations.

3.3 Mechanical Simulations

The main focus of the mechanical simulations was to review and optimize the effects of the size properties of the parts in terms of the resonance frequency.

Evaluation of the thickness, length, and width of the magnetostrictive material and how it affects the targeted resonance frequency value of the system was aimed during bending movement and aimed to provide an optimization. The desired resonance frequency between 700-1000 Hz was determined by inspiring previous bone conduction transducer studies[47].

In addition, meshing adjustments were optimized to get more consistent results during simulations. First, the system's resonance frequency was calculated by performing eight modes of modal and harmonic response analysis through ANSYS® Mechanical.

3.4 Electromagnetic Simulations

Some adjustments were made before running electromagnetic simulations. First, the coil's winding excitation was adjusted, and it was decided to proceed with a sinusoidal voltage source.

$$\textbf{Voltage} = V_m \sin(2\pi f t) \longrightarrow \textbf{Voltage} = 2\sin(2\pi 1000 t)$$

The next step was to calculate the coil's resistance, inductance and the number of conductors, and wire diameter, while the resistance and inductance values of the coil. Furthermore, copper resistivity and cross-sectional area of the coil were considered while calculating in resistance of the coil. Mesh settings were optimized after the settings of excitation of winding were completed. The optimized calculations of resistance and inductance with wire diameter and the number of turns of the coil are listed in Table 3.2. There were nine configurations for simulations.

Table 3.2: Calculated resistance and inductance value of coil.

Simulation Configurations	Permanent Magnet	Turns	Resistance	Inductance(μH)	Wire Diameter
1	N52	200	$9.34566e^{-8}$	5.4	0.81 mm
2	N52	225	$1.05139e^{-7}$	6.8	0.81 mm
3	N52	250	$1.16821e^{-7}$	8.4	0.81 mm
4	N50	200	$9.34566e^{-8}$	5.4	0.81 mm
5	N50	225	$1.05139e^{-7}$	6.8	0.81 mm
6	N50	250	$1.16821e^{-7}$	8.4	0.81 mm
7	N48	200	$9.34566e^{-8}$	5.4	0.81 mm
8	N48	225	$1.05139e^{-7}$	6.8	0.81 mm
9	N48	250	$1.16821e^{-7}$	8.4	0.81 mm

There were three different types of Silicon Core Iron Alloy for counterweight with different permeability values added to test combinations to review how different material permeability affects the bender's average magnetic field density in the transducer depending on the input voltage. In addition, there were three different thicknesses of a magnetostrictive alloy selected to review how different thicknesses of the material affect average magnetic field density depending on the input voltage. These thicknesses were selected in terms of mechanical simulation results.

Lastly, each of three different magnetostrictive materials with the same thickness was simulated as electromagnetic to investigate how different magnetic permeability affects the average magnetic field density of the bender in the transducer depending on the input voltage.

Nine simulation configurations, see in Table 3.3, were performed, including three different permanent magnets and three different coil turn numbers for each combination, and a total of sixty-three simulations were performed for all the test configurations in Table 3.4.

Table 3.3: Test configurations with materials for electromagnetic simulations.

Test Configurations	Magnetostrictive Material	Counterweight	The thickness of Magnetostrictive Material
A	Galfenol	Silicon Core Iron A	0.5 mm
B	Galfenol	Silicon Core Iron A	0.4 mm
C	Galfenol	Silicon Core Iron A	0.3 mm
D	Galfenol	Silicon Core Iron B	0.5 mm
E	Galfenol	Silicon Core Iron C	0.5 mm
F	Terfenol D	Silicon Core Iron A	0.5 mm
G	Metglas 2714A	Silicon Core Iron A	0.5 mm

4

Results

This chapter is focused on the results and comparisons of mechanical and electromagnetic simulations.

4.1 Mechanical Simulations

The following three cases focused on the effect of the width of the bender in the transducer on the resonance frequency. The parameters were kept the same apart from the width, and Galfenol alloy was used for these comparisons. All mechanical cases were reviewed in the eight different modes which are the transducer system's movement patterns oscillating at the resonance frequency.

Case 1

Material	Width	Thickness	Depth
Galfenol	20 mm	0.4 mm	4.8 mm

Table 4.1: Natural frequency results for Case 1.

Mode	1	2	3	4	5	6	7	8
Frequency [Hz]	609.22	864.71	1772.5	2272.8	4647.4	6488.7	9037.3	12388

Case 2

Material	Width	Thickness	Depth
Galfenol	16.5 mm	0.4 mm	4.8 mm

Table 4.2: Natural frequency results for Case 2.

Mode	1	2	3	4	5	6	7	8
Frequency [Hz]	984.11	1119.2	2273.3	3287	6536.2	9325.9	13349	17510

Case 3

Material	Width	Thickness	Depth
Galfenol	24 mm	0.4 mm	4.8 mm

Table 4.3: Natural frequency results for Case 3.

Mode	1	2	3	4	5	6	7	8
Frequency [Hz]	408.4	604.5	1450.2	1932	3230.2	4799	7699.4	9921.2

The subsequent three cases focused on the effect of the depth of magnetostrictive material on the resonance frequency.

Case 4

Material	Width	Thickness	Depth
Galfenol	20 mm	0.4 mm	7.8 mm

Table 4.4: Natural frequency results for Case 4.

Mode	1	2	3	4	5	6	7	8
Frequency [Hz]	557.4	884.28	1195.8	2330.7	3305.4	6606.9	9722.9	12495

C**ase 5**

Material	Width	Thickness	Depth
Galfenol	20 mm	0.4 mm	4.8 mm

Table 4.5: Natural frequency results for Case 5.

Mode	1	2	3	4	5	6	7	8
Frequency [Hz]	609.22	864.71	1772.5	2272.8	4647.4	6488.7	9037.3	12388

Case 6

Material	Width	Thickness	Depth
Galfenol	20 mm	0.4 mm	3.8 mm

Table 4.6: Natural frequency results for Case 6.

Mode	1	2	3	4	5	6	7	8
Frequency [Hz]	619.69	861.81	2111.9	2240.2	5400	6384.3	8484.9	12514

Six cases were listed to focus on the effect of the width and depth parameters of the bender in the transducer on the resonance frequency from the mechanical simulations listed above. Eighteen simulations were performed and illustrated as the most consistent simulation data above. The resonance frequency decreased as the length of the magnetostrictive material increased, and there was no direct correlation between the depth of the material and the resonance frequency.

The following three cases focused on comparing the resonance frequency of different three magnetostrictive materials with a thickness of 0.3 mm.
The effect of different magnetostrictive materials on the resonance frequency was observed. Hence, parameters were kept the same apart from the thickness.

Case 7

A bending movement of the bone conduction transducer, which includes Galfenol alloy as bender, was seen in the second mode at 685.07 Hz. Observed all-natural frequencies were listed in Table 4.1, and the bending movements and harmonic response analysis of the model were shared in Figures 4.1 and 4.2.

Table 4.7: Natural frequency results for Case 7.

Mode	1	2	3	4	5	6	7	8
Frequency [Hz]	461.8	685.07	1319.9	2096.6	4375.4	6208	8940.2	11913

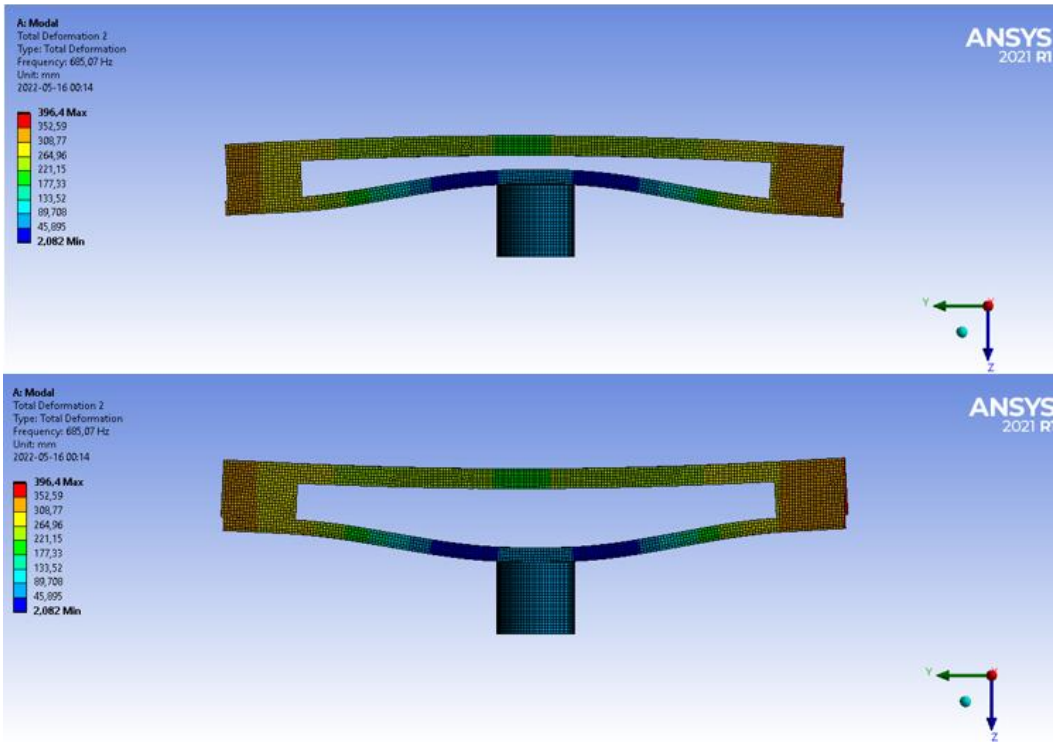

Figure 4.1: The bending motion of the transducer model at 685.07 Hz.

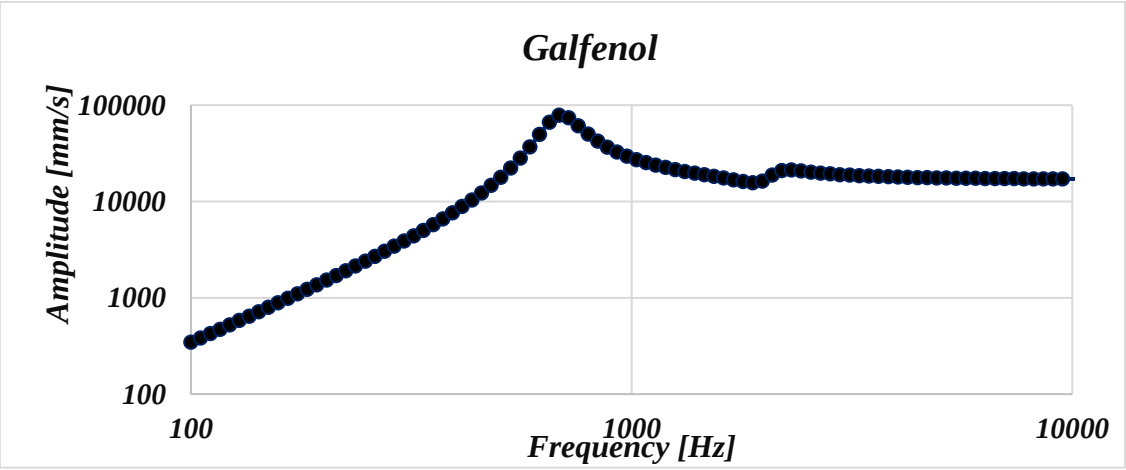

Figure 4.2: Harmonic response analysis of the model in Case 7.

Case 8

Terfenol D was used for this case, and the bending motion of the transducer was observed in the second mode at 603.13 Hz. The acquired natural frequencies are listed in Table 4.2.

Furthermore, the transducer model's bending movements and harmonic response analysis are shown in Figures 4.3 and 4.4.

Table 4.8: Natural frequency results for Case 8.

Mode	1	2	3	4	5	6	7	8
Frequency [Hz]	399.97	603.13	1131	2039.9	4305.2	6125.9	8939.6	11805

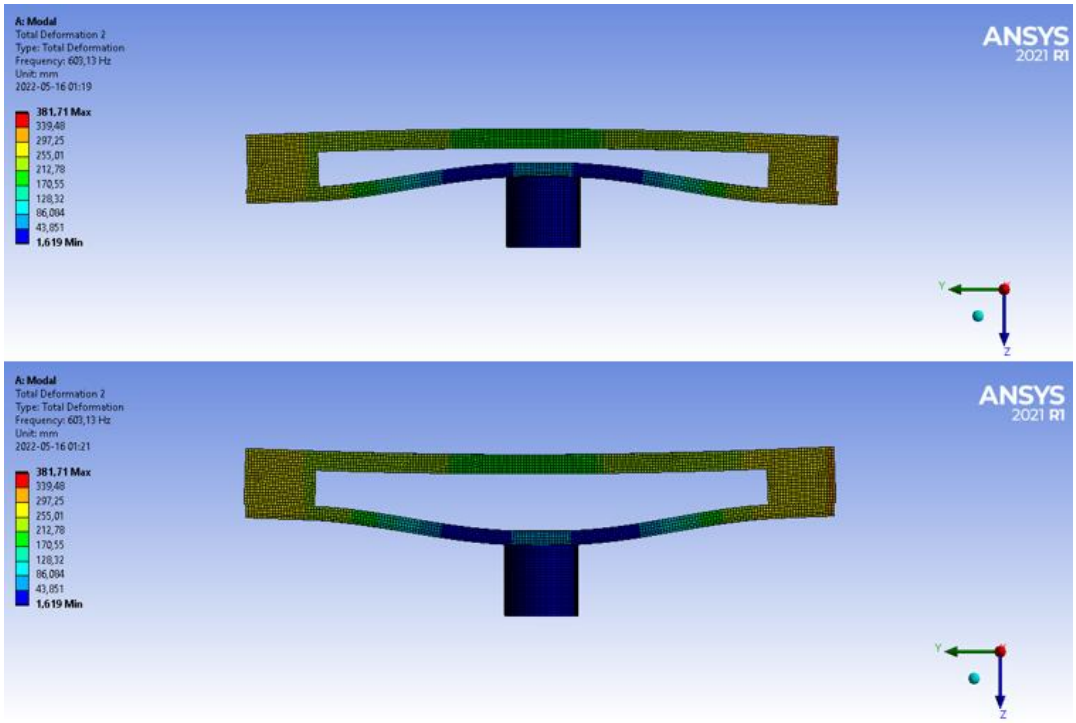

Figure 4.3: The bending motion of the transducer model at 603.13 Hz.

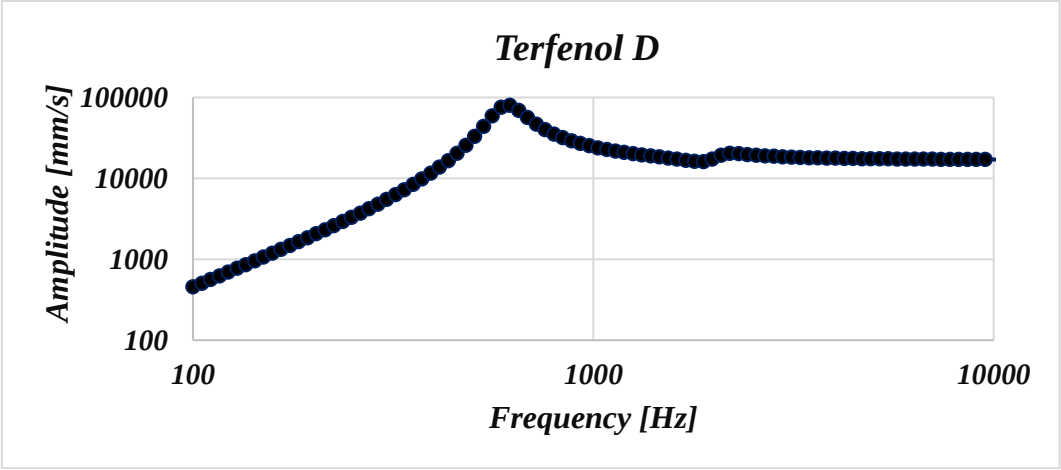

Figure 4.4: Harmonic response analysis of Case 8.

Case 9

This case included Metglas2714A magnetic alloy as a magnetostrictive material. The bending motion of the bone conduction transducer model was seen in the second mode at 756.17 Hz.

The observed natural frequencies were listed in Table 4.3, and the bending movements and harmonic response analysis of the model were shared in Figures 4.5 and 4.6.

Table 4.9: Natural frequency results for Case 9.

Mode	1	2	3	4	5	6	7	8
Frequency [Hz]	517.1	756.17	1527.9	2153.4	4461.2	6287.8	8940.7	12003

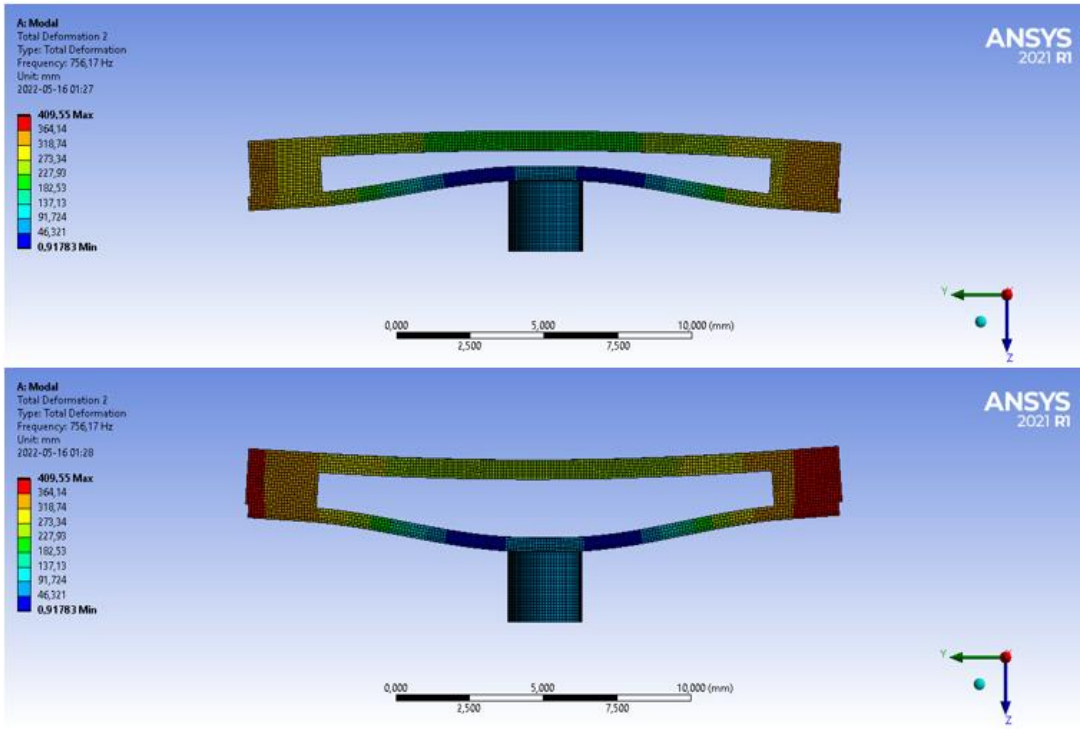

Figure 4.5: The bending motion of the transducer model at 603.13 Hz.

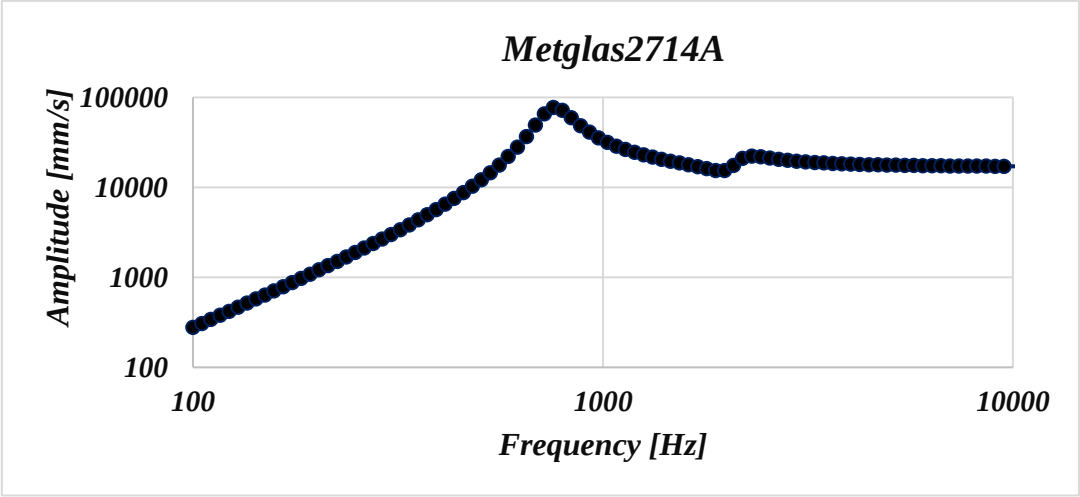

Figure 4.6: Harmonic response analysis of Case 9.

The following three cases focused on comparing the resonance frequency of different three magnetostrictive materials with a thickness of 0.4 milimeter. The effect of different magnetostrictive materials on the resonance frequency was observed.

Case 10

This case was performed for Galfenol, and the bending movement of the bone conduction transducer model was seen in the second mode at 864.71 Hz. The observed natural frequencies are listed in Table 4.4, and the bending movements and harmonic response analysis of the model are shown in Figures 4.7 and 4.8.

Table 4.10: Natural frequency results for Case 10.

Mode	1	2	3	4	5	6	7	8
Frequency [Hz]	609.22	864.71	1772.5	2272.8	4647.4	6488.7	9037.3	12388

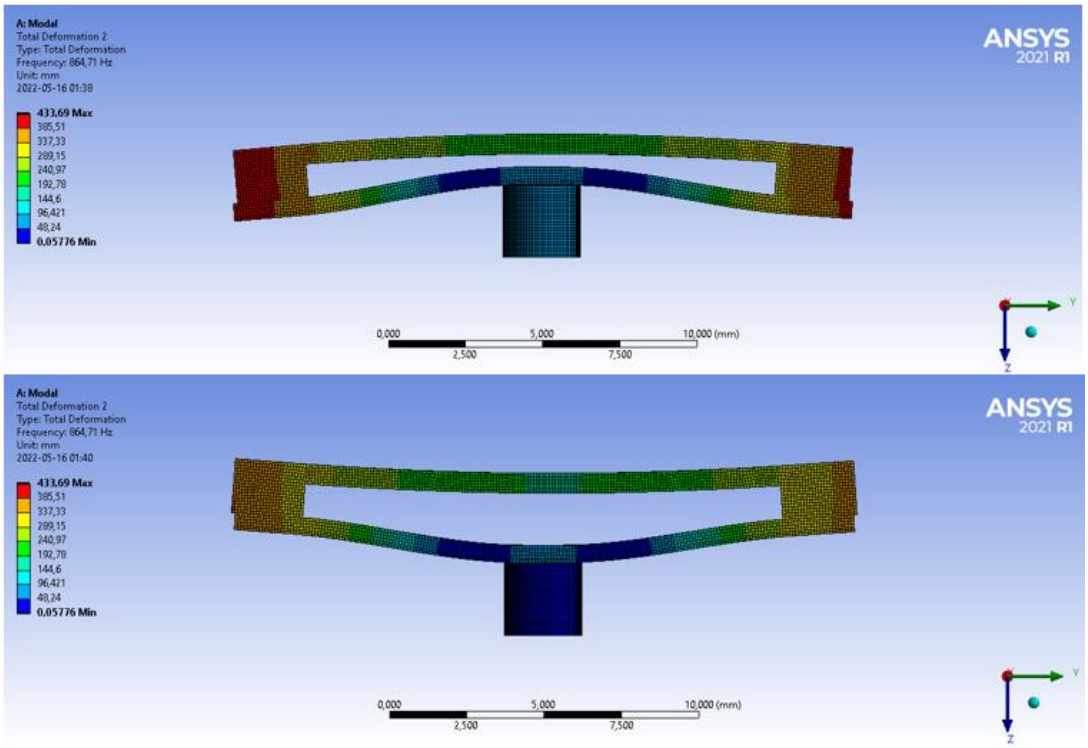

Figure 4.7: The bending motion of the transducer model at 864.71 Hz.

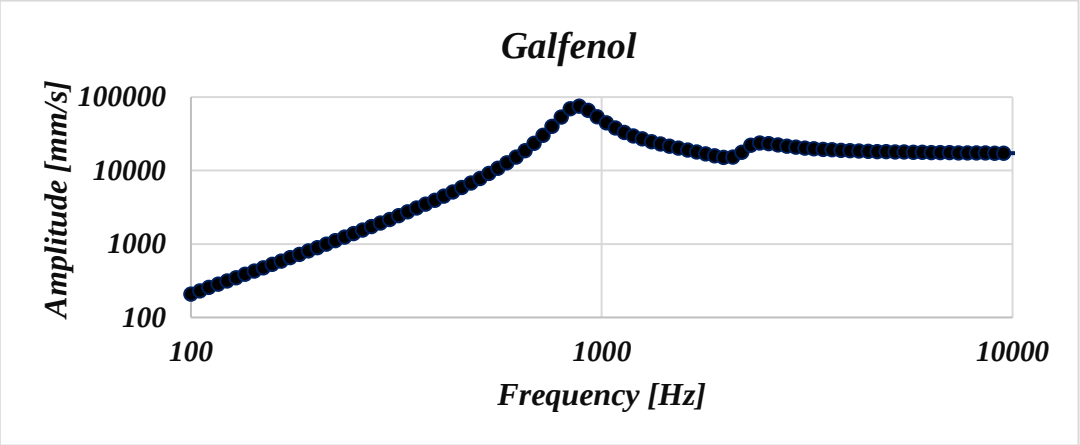

Figure 4.8: Harmonic response analysis of Case 4.

Case 11

Case 11 focused on the Terfenol D, and the bending movement of the bone conduction transducer model was seen in the second mode at 763.64 Hz. The observed natural frequencies were listed in Table 4.5, and the bending movements and harmonic response analysis of the model were shared in Figures 4.9 and 4.10.

Table 4.11: Natural frequency results for Case 11.

Mode	1	2	3	4	5	6	7	8
Frequency [Hz]	525.55	763.64	1512.9	2181.1	4526.3	6355.5	9036.6	12216

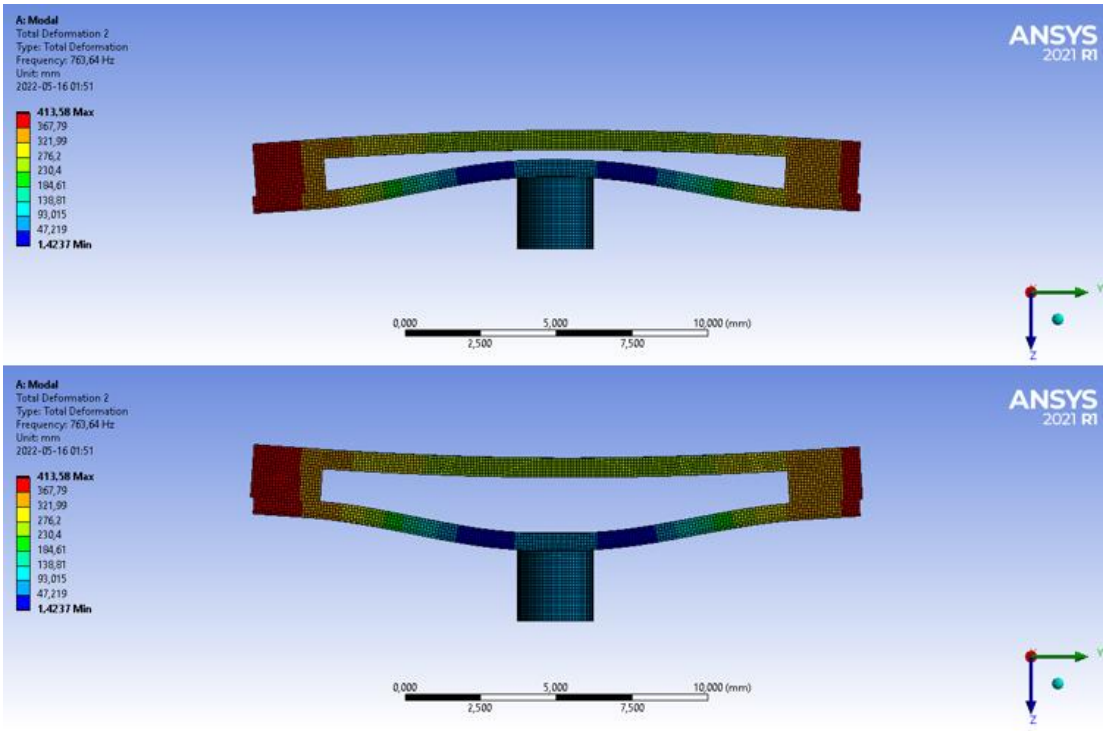

Figure 4.9: The bending motion of the transducer model at 763.64 Hz.

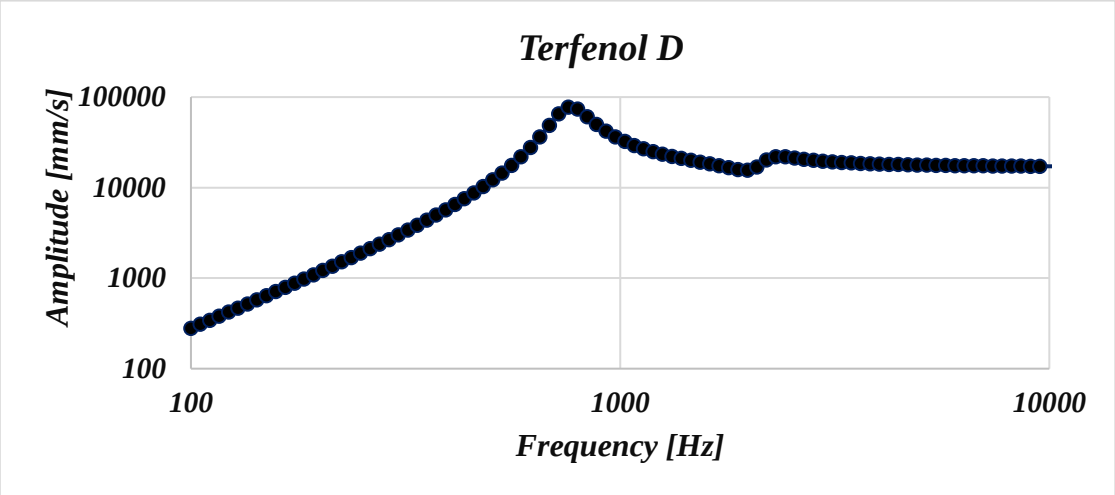

Figure 4.10: Harmonic response analysis of Case 11.

Case 12

Metglas2714A was used in this case, and the bending movement of the bone conduction transducer model was seen in the second mode at 959.22 Hz. The observed natural frequencies were listed in Table 4.6, and the bending movements and harmonic response analysis of the model were shown in Figures 4.11 and 4.12.

Table 4.12: Natural frequency results for Case 12.

Mode	1	2	3	4	5	6	7	8
Frequency [Hz]	688.52	959.22	2076.4	2378.3	4859.7	6669.1	9106.8	12661

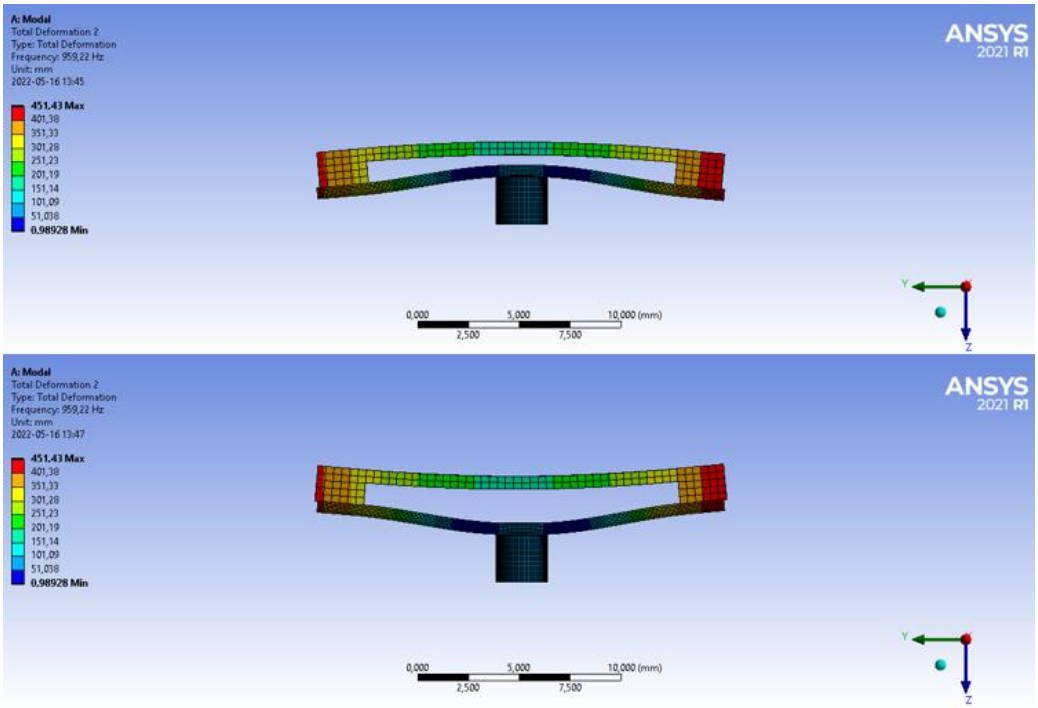

Figure 4.11: The bending motion of the transducer model at 959.22 Hz.

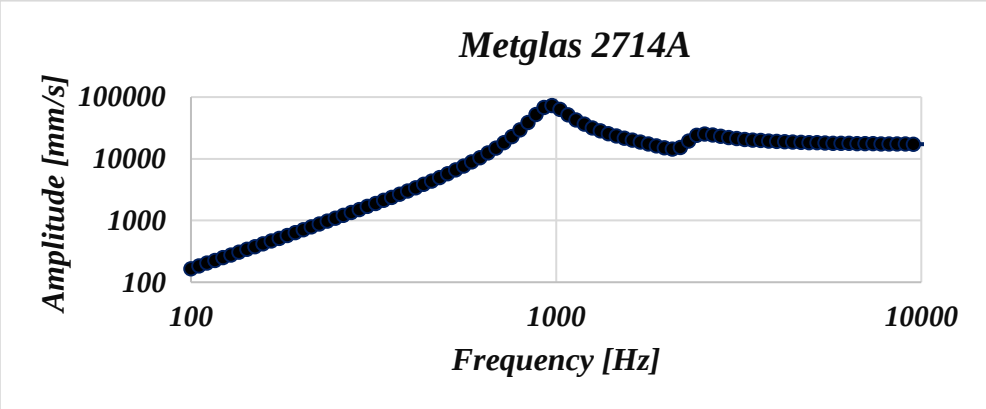

Figure 4.12: Harmonic response analysis of Case 12.

The following three cases focused on comparing the resonance frequency of different three magnetostrictive materials with a thickness of 0.5 milimeter. The effect of different magnetostrictive materials on the resonance frequency was observed.

Case 13

This case was performed for Galfenol, and the bending motion of the model was seen in the second mode at 1043.5 Hz. The observed natural frequencies were listed in Table 4.7, and the bending movements and harmonic response analysis of the model were shared in Figures 4.13 and 4.14.

Table 4.13: Natural frequency results for Case 13.

Mode	1	2	3	4	5	6	7	8
Frequency [Hz]	764.43	1043.5	2262.8	2486.2	5035.5	6856.2	9213.3	13033

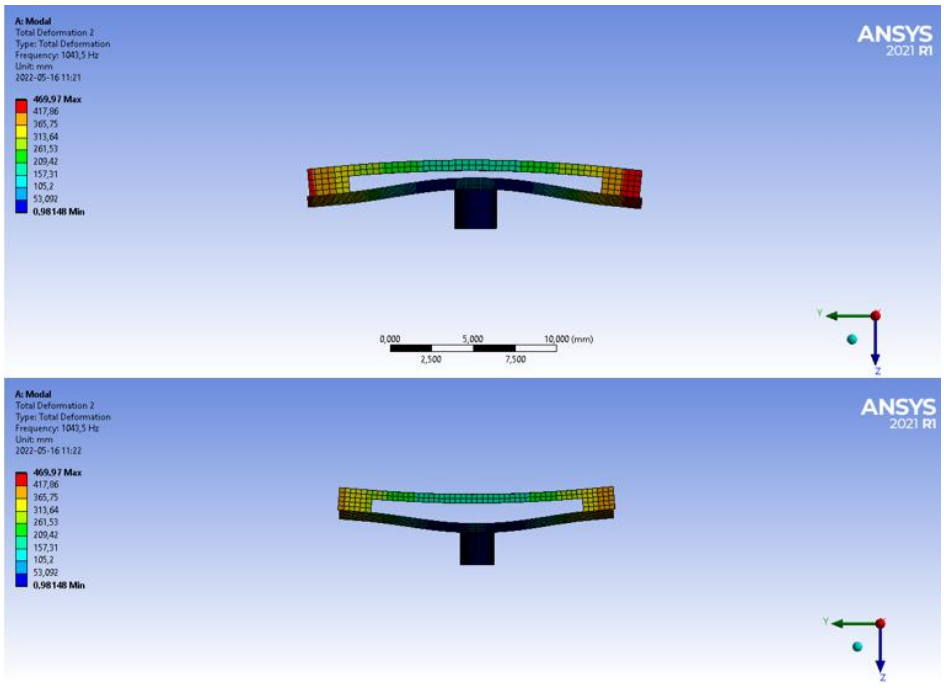

Figure 4.13: The bending motion of the transducer model at 1043.5 Hz.

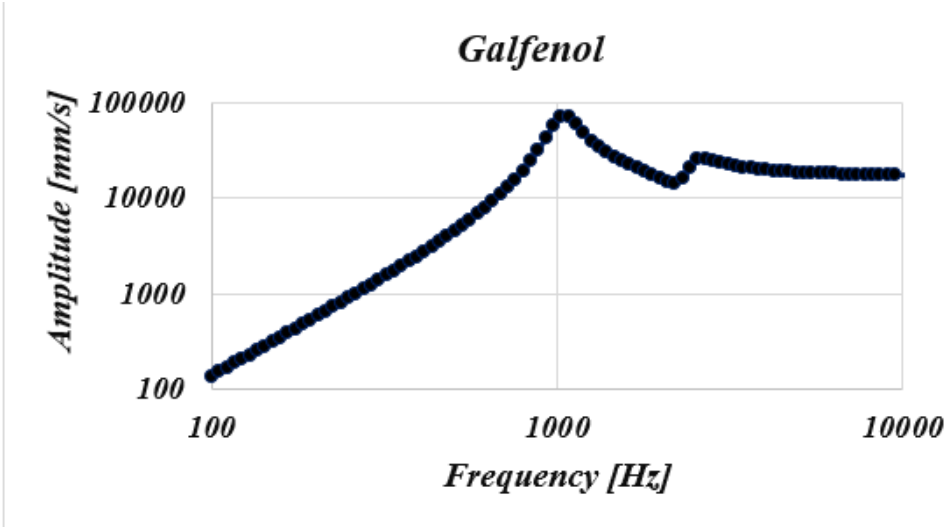

Figure 4.14: Harmonic response analysis of Case 13.

Case 14

Terfenol D was used for this case, and the bending movement of the bone conduction transducer model was seen in the second mode at 922.47 Hz. The observed natural frequencies were listed in Table 4.8, and the bending movements and harmonic response analysis of the model were shown in Figures 4.15 and 4.16.

Table 4.14: Natural frequency results for Case 14.

Mode	1	2	3	4	5	6	7	8
Frequency [Hz]	656.46	922.47	1922.2	2354.4	4847.4	6660	9212.2	12777

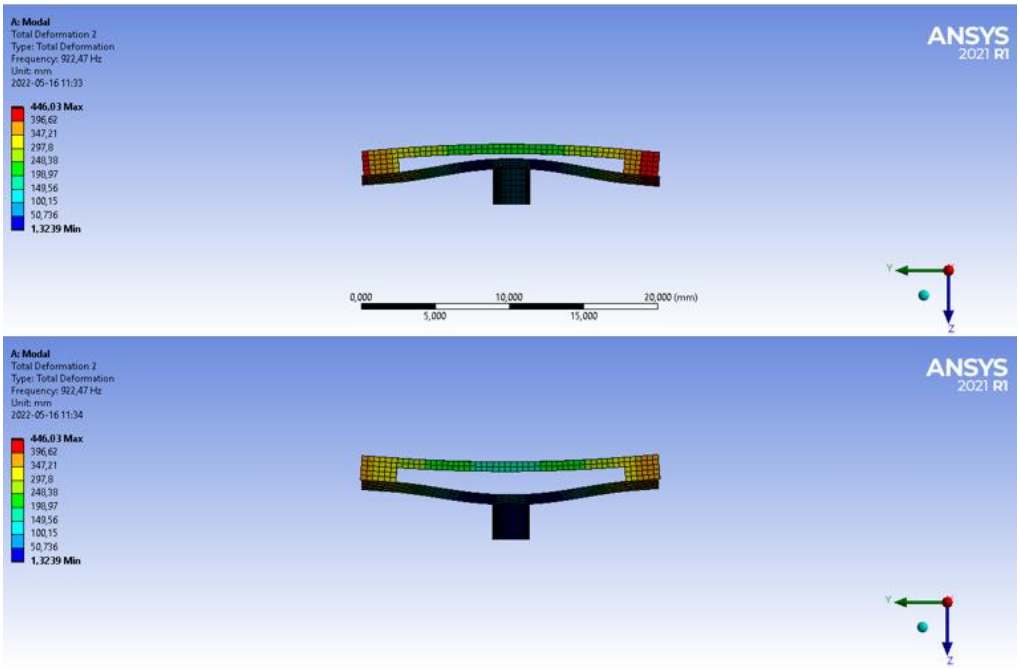

Figure 4.15: The bending motion of the transducer model at 922.47 Hz.

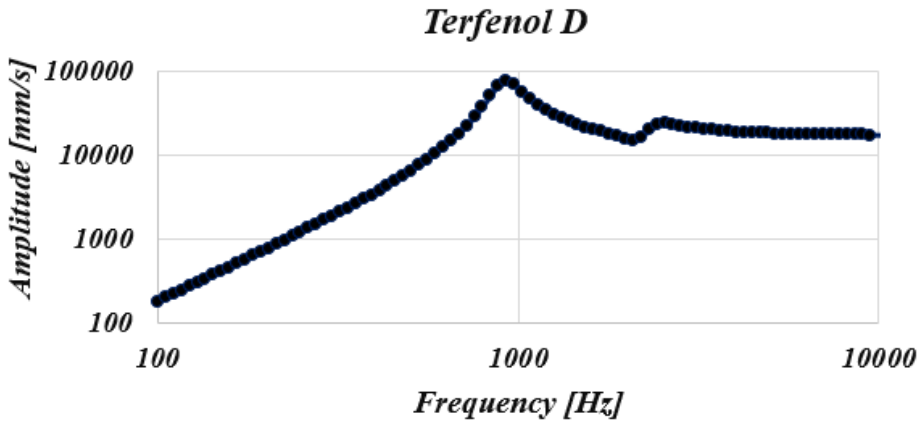

Figure 4.16: Harmonic response analysis of Case 14.

Case 15

Metglas 2714A Magnetic alloy was used, and the bending motion of the model was seen in the second mode at 1157.6 Hz.

The observed natural frequencies were listed in Table 4.9, and the bending movements and harmonic response analysis of the model were seen in Figures 4.17 and 4.18.

Table 4.15: Natural frequency results for Case 15.

Mode	1	2	3	4	5	6	7	8
Frequency [Hz]	868.54	1157.6	2622.3	2670	5289.7	7061.4	9214.6	13289

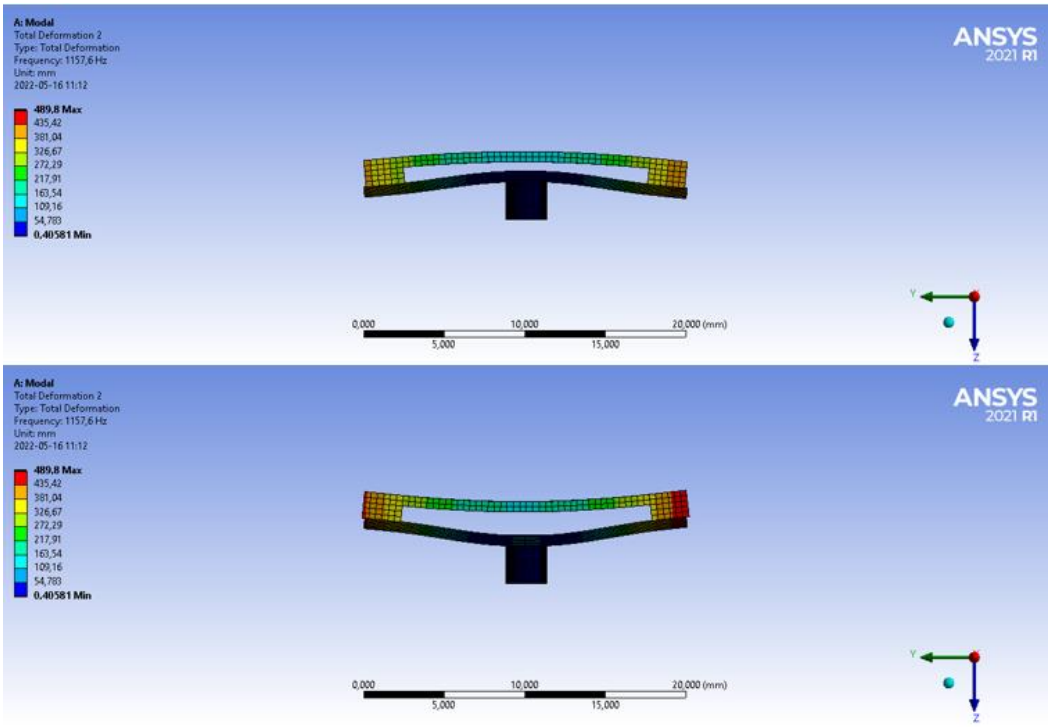

Figure 4.17: The bending motion of the transducer model at 1157.6 Hz.

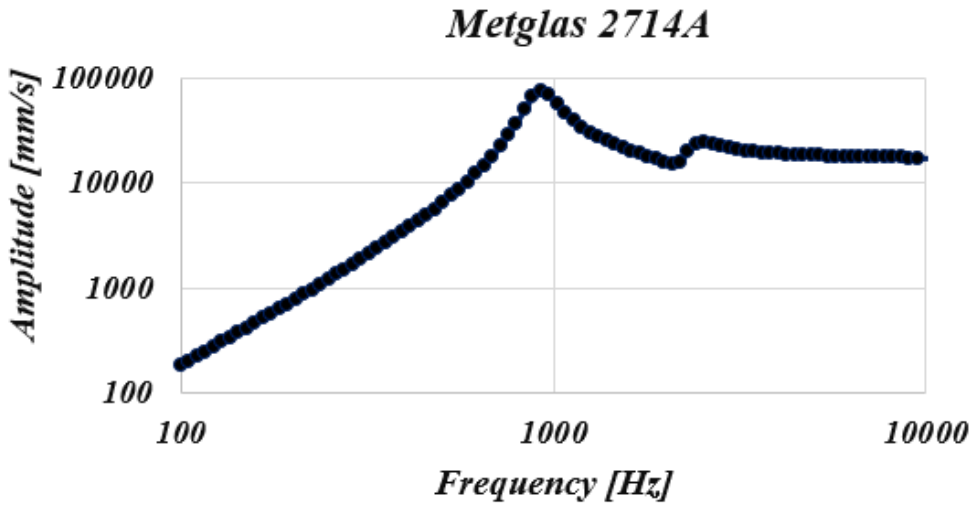

Figure 4.18: Harmonic response analysis of Case 15.

According to the views from mechanical simulations, the resonance frequency during bending movement increased as the thickness of the magnetostrictive material increased, and the bending movement of the transducer was observed in second modes for all simulations.

For the thickness of 0.3 mm, only Metglas 2714A ensured a desired level in the resonance frequency is being between 700 Hz and 1000 Hz. All three ferromagnetic materials with a thickness of 0.4 mm were ensured in the resonance frequency range. For the thickness of 0.5 mm, Metglas 2714A, Terfenol D and Galfenol ensured the resonance frequency range.

4.2 Electromagnetic Simulations

Electromagnetic simulations were performed through ANSYS Electronics, and Maxwell 2D was preferred to be a more effective computation in terms of time and cost. In addition, the 2D model was preferred since the bending moment of the model occurred on only one axis.

The following three cases compared the average magnetic field density of bender in transducer for the same magnetostrictive material for different thicknesses.

Case 1

Parameters	Permanent Magnet	Turns of Coil	Resistance Value	Inductance Value (μH)	Voltage Excitation
Selection	N52	200	$9.34566e^{-8}$	5.4	2*sin(2*pi*1000*time)

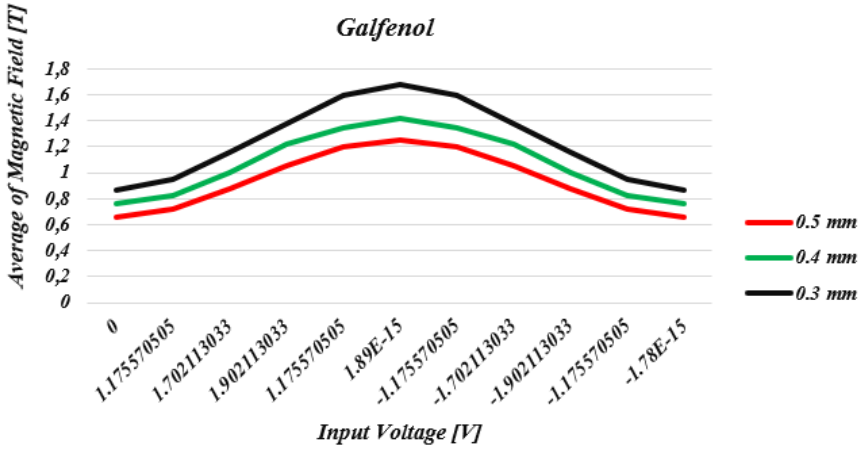

Figure 4.19: Comparisons of average magnetic field density same magnetostrictive material for different thicknesses.

Case 2

Parameters	Permanent Magnet	Turns of Coil	Resistance Value	Inductance Value (μH)	Voltage Excitation
Selection	N50	225	$1.05139e^{-7}$	6.8	2*sin(2*pi*1000*time)

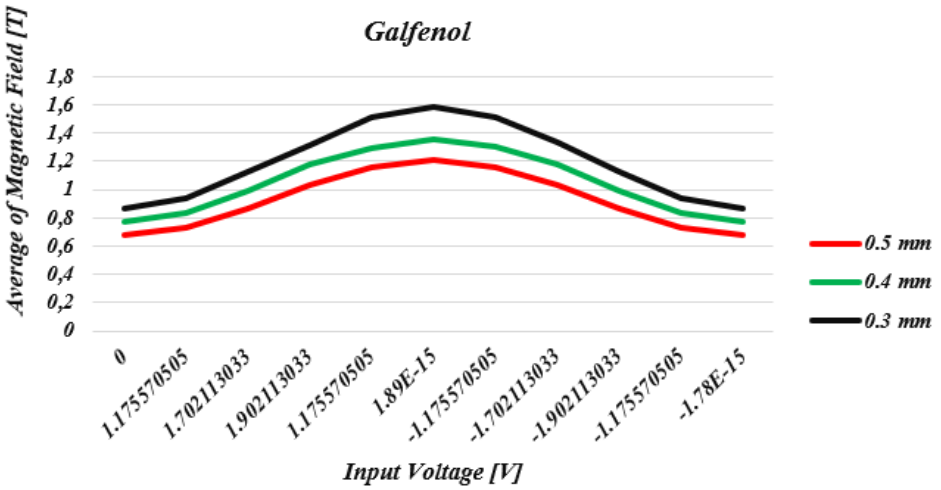

Figure 4.20: Comparisons of average magnetic field density same magnetostrictive material for different thicknesses.

Case 3

Parameters	Permanent Magnet	Turns of Coil	Resistance Value	Inductance Value (μH)	Voltage Excitation
Selection	N48	250	$1.16821e^{-7}$	8.4	2*sin(2*pi*1000*time)

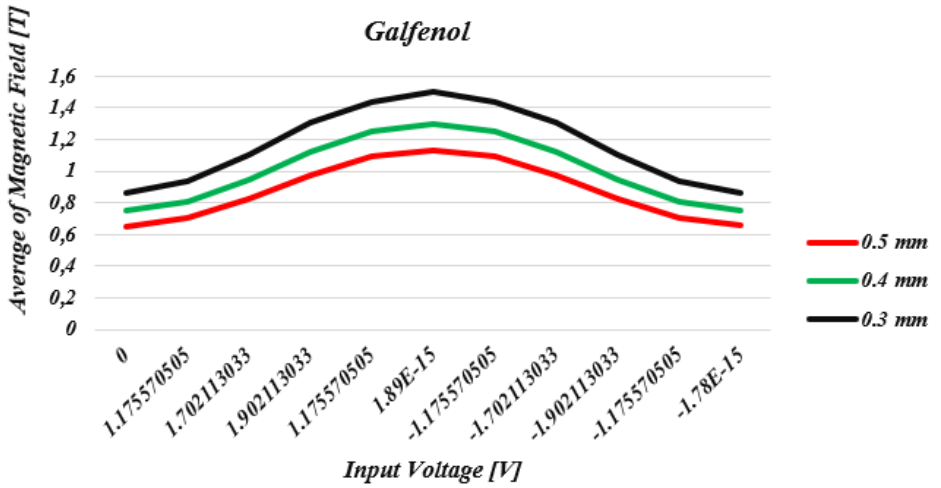

Figure 4.21: Comparisons of average magnetic field density same magnetostrictive material for different thicknesses.

The thickness of magnetostrictive material decreased as the average magnetic field density of the bender in the transducer increased.

The subsequent three cases focused on comparing the average magnetic field density of different counterweight materials with the same thickness of magnetostrictive material.

Case 4

Parameters	Permanent Magnet	Turns of Coil	Resistance Value	Inductance Value (µH)	Voltage Excitation
Selection	N52	200	$9.34566e^{-8}$	5.4	2*sin(2*pi*1000*time)

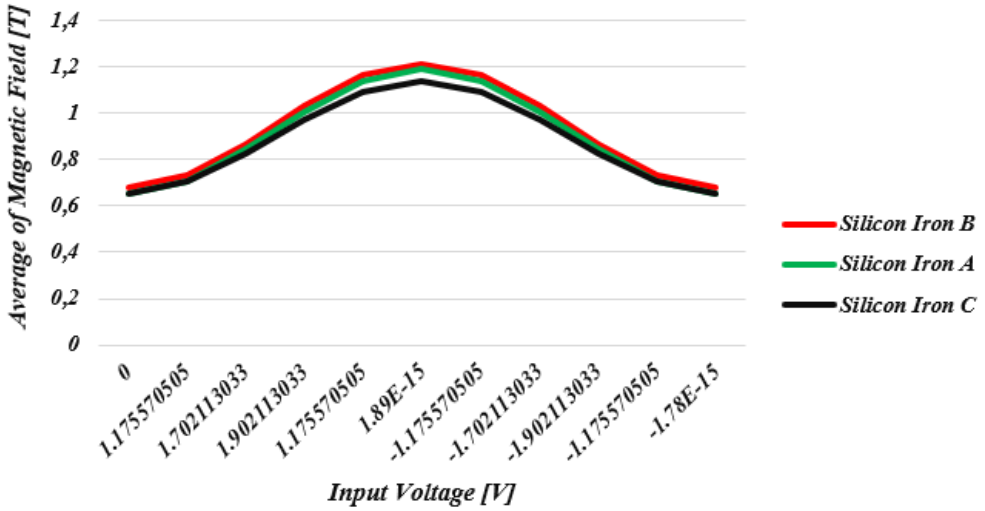

Figure 4.22: Comparisons of average magnetic field density same magnetostrictive material for different permeabilities of counterweight.

Case 5

Parameters	Permanent Magnet	Turns of Coil	Resistance Value	Inductance Value (µH)	Voltage Excitation
Selection	N50	225	$1.05139e^{-7}$	6.8	2*sin(2*pi*1000*time)

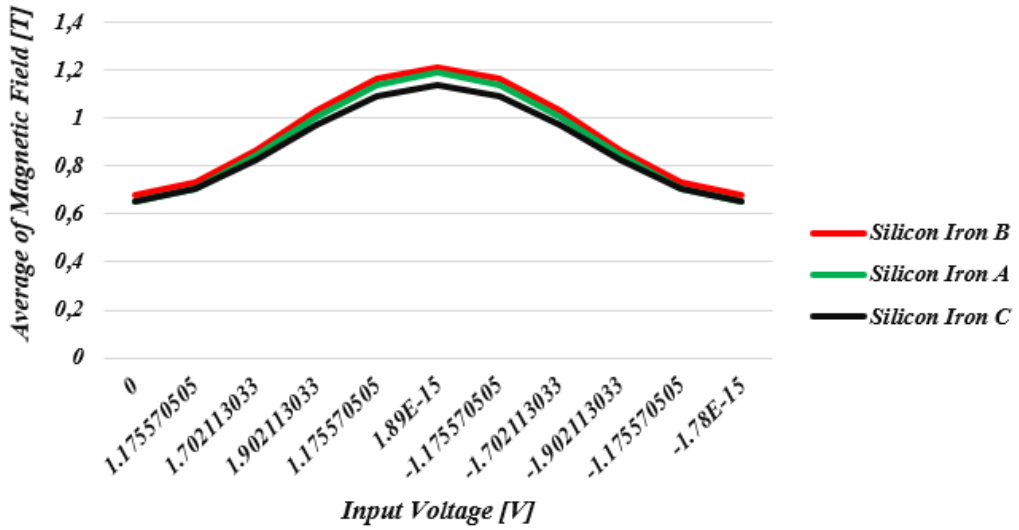

Figure 4.23: Comparisons of average magnetic field density same magnetostrictive material for different permeabilities of counterweight.

Case 6

Parameters	Permanent Magnet	Turns of Coil	Resistance Value	Inductance Value (μH)	Voltage Excitation
Selection	N48	250	$1.16821e^{-7}$	8.4	2*sin(2*pi*1000*time)

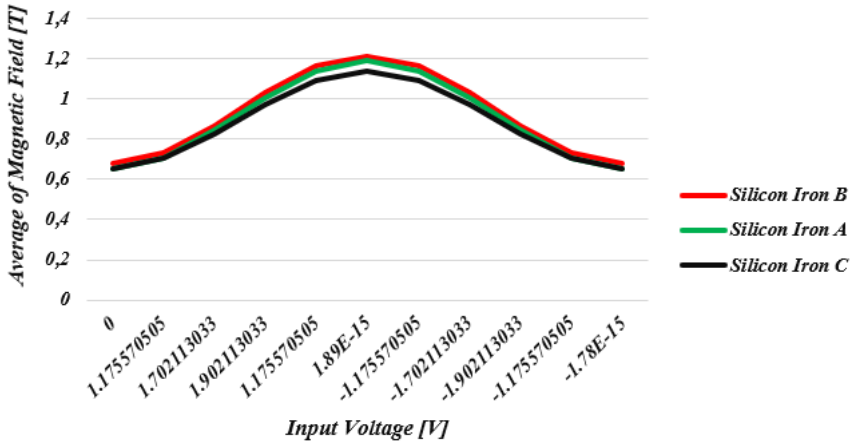

Figure 4.24: Comparisons of average magnetic field density same magnetostrictive material for different permeabilities of counterweight.

The average magnetic field density of the bender was observed to increase as the permeability of the counterweight material. However, it was noticed that the effect of the differences between material permeability is pretty low for counterweight.

Following three cases compared the effect of Terfenol D, Metglas 2714A, and Galfenol alloys for the average magnetic field density of the bender.

Case 7

Parameters	Permanent Magnet	Turns of Coil	Resistance Value	Inductance Value (μH)	Voltage Excitation
Selection	N52	200	$9.34566e^{-8}$	5.4	2*sin(2*pi*1000*time)

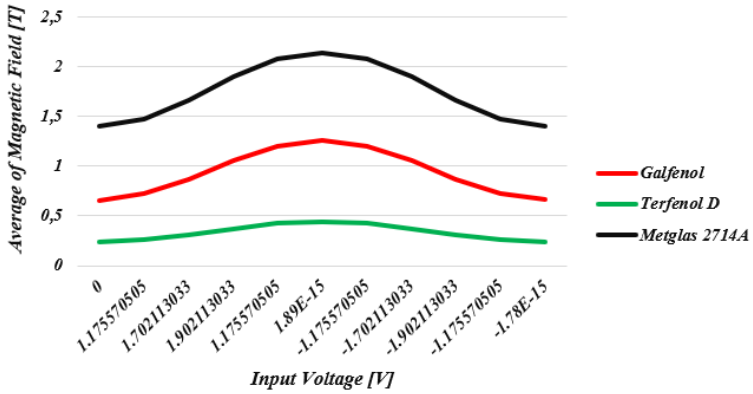

Figure 4.25: Comparisons of average magnetic field density of different magnetostrictive materials.

Case 8

Parameters	Permanent Magnet	Turns of Coil	Resistance Value	Inductance Value (μH)	Voltage Excitation
Selection	N50	250	1,16821e^{-7}	8.4	2*sin(2*pi*1000*time)

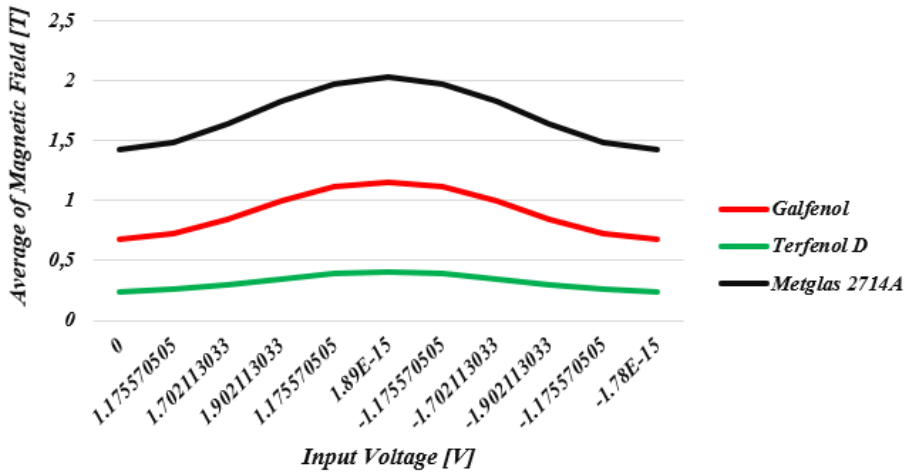

Figure 4.26: Comparisons of average magnetic field density of different magnetostrictive materials.

Case 9

Parameters	Permanent Magnet	Turns of Coil	Resistance Value	Inductance Value (μH)	Voltage Excitation
Selection	N48	250	1.16821e^{-7}	8.4	2*sin(2*pi*1000*time)

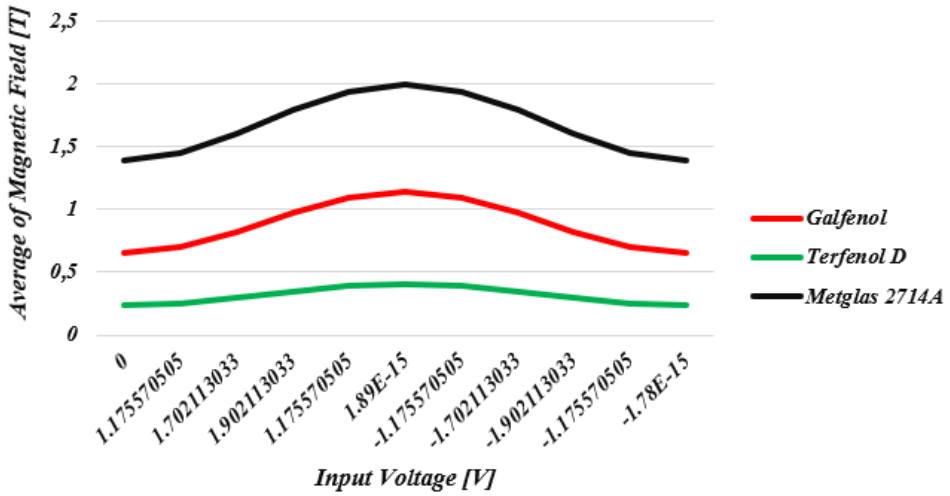

Figure 4.27: Comparisons of average magnetic field density of different magnetostrictive materials.

The magnetostrictive effect of the Metglas 2714A alloy was pretty high compared to the other two alloys. On the other hand, it was determined that the effect of the Terfenol-D alloy was much less than the Galfenol and Metglas 2714A alloy.

5

Discussion

This paper focused on each of the previous mechanical and electromagnetic simulation cases. Then, the obtained results and methodology of them will be based on regarded studies.

5.1 Mechanical Studies

Figure 5.1 is aimed to see how the material properties affect the resonance frequency.

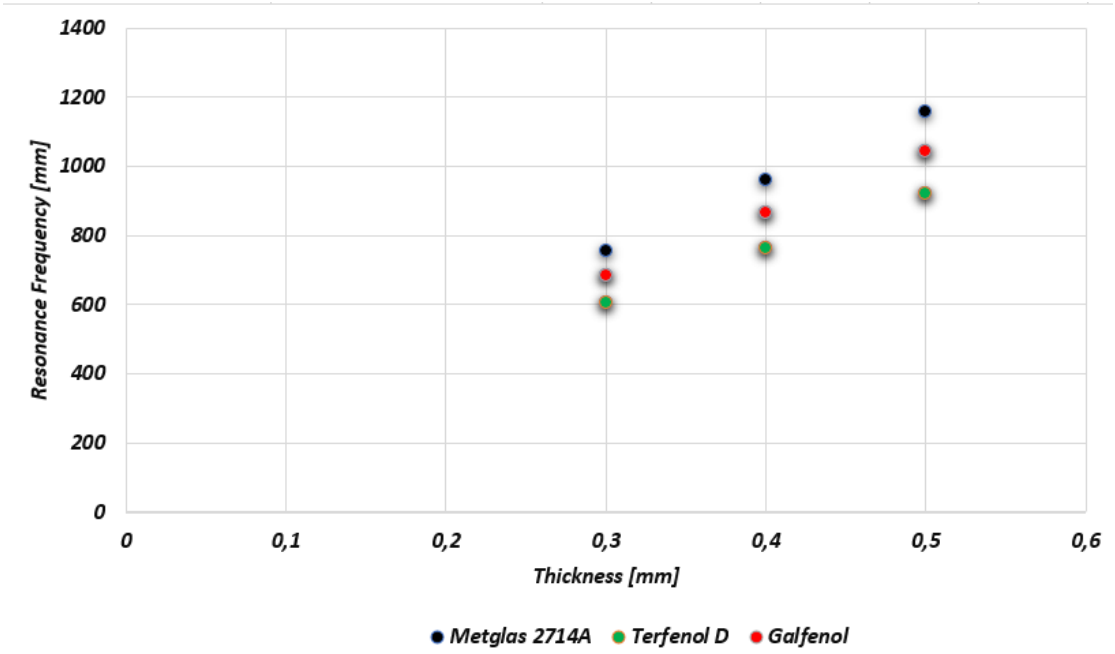

Figure 5.1: The figure illustrates how the material properties affect the resonance frequency.

According to the data, the materials with the highest resonance frequency are listed from largest to smallest as Metglas 2714A, Galfenol, and Terfenol D alloys during bending. This correlation arises from the direct proportion between Young's modulus and the natural frequency [48]. Furthermore, Young's modulus of materials is sorted from highest to lowest as Metglas 2714A, Galfenol, and Terfenol D alloys [40][49]. Therefore, different material properties -excluding Young's modulus- can be investigated for other effects. Also, Figures 5.1 can show to see how the thickness affects the resonance frequency. The design with the thickest magnetostrictive material presented the highest resonance frequency according to the obtained data. Therefore, this argument can be based on the magnetostrictive material thickness directly correlates with the system's resonance frequency[50]. Another significant point is the relationship between length and resonance frequency. It was found that the resonance frequency decreases as the length of the magnetostrictive material increases. It is thought that this correlation is based on the resonance frequency being inversely proportional to the length[51].

A proper relationship between the depth of material and resonance frequency was not observed; however, this can be more investigated in another study.

Some alloys did not provide targeted resonance frequency criteria. For 0.3 mm, the resonance frequency of Galfenol and Terfenol D was pretty low, but Metglas 2714A had satisfactory results. For 0.4 mm, all three magnetostrictive materials provided a desired resonance frequency range. For 0.5 mm, the resonance frequency of Metglas 2714A was not suitable because of a higher frequency than the specified range. Galfenol and Terfenol D had desired data for 0.5 mm. Although the consistent results of Terfenol D, it was considered that Terfenol D should not be recommended for building possible prototype studies due to its high fragility[52]. It should not be forgotten that a transducer model does not have to be precise in these dimensions. However, there were sufficient dimensions to build a magnetostrictive transducer prototype because it gets the correct resonance frequency and gives similar sizes to comparable existing bone conduction transducers. Hence, these can be evaluated as reasonable.

5.2 Electromagnetic Studies

Metglas 2714A had the highest average magnetic field density of the bender in the transducer, which was observed when the thicknesses were kept the same, and, Galfenol had an average magnetic field density higher than Terfenol D in the same conditions. This correlation is thought to be based on the magnetic permeability property of the materials because the magnetic permeability of Metglas2714 A was more than Galfenol and Terfenol D [53]. Furthermore, this observation can be related to the ferromagnetic material's smaller magnetic saturation field, causing a more magnetic permeability [54]. average magnetic field of the bender in the transducer. The average magnetic field density increased while increasing the magnetic permeability of the counterweight material because magnetic permeability has a direct correlation to magnetic field density. However, it was pretty remarkable that this effect was low.

A demagnetization situation was thought of as another significant point. Demagnetization can occur if the average magnetic field density exceeds the magnetic saturation value of ferromagnetic material. The average magnetic field density of three alloys with a thickness of 0.3 mm exceeds magnetic saturation values. For 0.4 mm, magnetic field densities were lower magnetic saturations but were pretty close to the magnetic saturation. Therefore, it is considered risky in demagnetization due to safety factors. However, there is no observed exceeding for ferromagnetic materials with 0.5 mm.

6

Conclusion

This thesis study aims to find a possible magnetostrictive transducer design and provide optimized data to build a possible magnetostrictive transducer for bone conduction use. Mechanical and electromagnetic simulations were performed through ANSYS®. According to the literature review, Metglas®2714A, Galfenol, and Terfenol D alloys are evaluated to use in a bone conduction transducer. There is desired resonance frequency was between around 700 – 1000 Hz.

The results showed that Galfenol alloy is quite pleasant to build a magnetostrictive prototype for bone conduction use. Metglas®2714A provides the necessary specified resonance frequency for 0.3 mm and 0.4 mm thickness and presents a higher magnetic field density than the other two alloys. In addition, it is more durable than the other two alloys. However, there is no commercial manufacturing of the desired thickness. Hence, it is not possible to use for building a prototype.

On the other hand, Terfenol D ensures the desired resonance frequency range for the thickness of 0.4 mm and 0.5 mm, but it is not be preferred because its fragility is pretty high and almost equal to piezo material. The magnetic field densities are lower than for the other two alloys. Furthermore, there is no commercial manufacturing lower than 0.762 mm.

Galfenol alloy has suitable resonance frequency results for 0.4 mm and 0.5 mm thickness. Also, the average magnetic field density results are pretty consistent. The thickness of 0.4 mm presents around 1.42 Tesla, the thickness of 0.5 mm 1.26 Tesla. Hence, Galfenol alloy with 0.5 mm was more acceptable than other thicknesses due to the demagnetization value and the safety factor criteria.

It is suggested to use Galfenol alloy with 0.5 mm thickness, 20 mm length, and 4.8 mm to build a magnetostrictive transducer prototype using a permanent neodymium magnet with 200-250 turns of the coil.

6.1 Future work

This thesis research provides a new perspective on building a magnetostrictive transducer for bone conduction use.

In a future step, a magnetostrictive transducer for bone conduction use can be constructed as a prototype based on the simulation results of this study and the performance level can be measured in terms of efficiency of force output, which may depend on the quality of the output signals. Furthermore, this prototype can also review the correlation between output force level and average magnetic field density of bender in bone conduction transducer. Finally, Metglas®2714A alloy can be reviewed again for magnetostrictive material for bone conduction use if there will be commercial manufacturing with suitable sizes.

7

Bibliography

[1] "Deafness and hearing loss," 2021. https://www.who.int/news-room/fact-sheets/detail/deafness-and-hearing-loss.

[2] O. Guillon *et al.*, "New considerations about the fracture mode of PZT ceramics," *J. Eur. Ceram. Soc.*, vol. 25, pp. 2421–2424, 2005, doi: 10.1016/j.jeurceramsoc.2005.03.074.

[3] M. Mozaffari, R. Nash, and A. S. Tucker, "Anatomy and Development of the Mammalian External Auditory Canal: Implications for Understanding Canal Disease and Deformity," *Front. Cell Dev. Biol.*, vol. 8, no. January, pp. 1–11, 2021, doi: 10.3389/fcell.2020.617354.

[4] Human Ear-Occupational Safety & Health Administration, "Human Ear," in *Occupational Safety & Health Administration*, 1999, p. Section III.

[5] B. B. Ballachanda, "The human ear canal," in *The human ear canal*, 1995th ed., 1995.

[6] E. A. G. Shaw, "Transformation of sound pressure level from the free field to the eardrum in the horizontal plane," *J. Acoust. Soc. Am.*, vol. 56, no. 6, pp. 1848–1861, 1974, doi: 10.1121/1.1903522.

[7] S. Kramer and D. K. Brown, "Audiology: Science to Practice, Third Edition," *Audiol. Sci. to Pract. Third Ed.*, p. 439, 2018, [Online]. Available: http://ezproxy.unal.edu.co/books/audiology-science-practice-third-edition/docview/2136055587/se-2?accountid=137090.

[8] S. Reinfeldt, *Bone Conduction Hearing in Human Communication .Sensitivity , Transmission , and Applications*. 2009.

[9] A. Mudry and A. Tjellström, "Historical background of bone conduction hearing devices and bone conduction hearing aids," *Adv. Otorhinolaryngol.*, vol. 71, pp. 1–9, 2011, doi: 10.1159/000323569.

[10] S. Stenfelt, "Acoustic and Physiologic Aspects of Bone Conduction Hearing," vol. 71, pp. 10–21, 2011.

[11] S. Stenfelt, "Middle ear ossicles motion at hearing thresholds with air conduction and bone conduction stimulation.," *J. Acoust. Soc. Am.*, vol. 119, no. 5 Pt 1, pp. 2848–2858, May 2006, doi: 10.1121/1.2184225.

[12] S. Stenfelt, "Middle ear ossicles motion at hearing thresholds with air conduction and bone conduction stimulation Middle ear ossicles motion at hearing thresholds with air conduction and bone conduction stimulation," no. May, 2014, doi: 10.1121/1.2184225.

[13] S. Reinfeldt, B. Håkansson, H. Taghavi, and M. Eeg-Olofsson, "New developments in bone-conduction hearing implants: A review," *Med. Devices Evid. Res.*, vol. 8, pp. 79–93, 2015, doi: 10.2147/MDER.S39691.

[14] C. Rigato and C. Rigato, *On Direct Drive Bone Conduction Devices*. 2019.

[15] B. O. Hakansson, A. Tjellstrom, U. L. F. Rosenhall, and P. Carlsson, "The Bone-Anchored Hearing Aid," no. 1, pp. 229–239, 1985.

[16] B. Håkansson, "The Future of Bone Conduction Hearing Devices," vol. 71, pp. 140–152, 2011.

[17] A. Magele, P. Schoerg, B. Stanek, B. Gradl, and G. M. Sprinzl, "Active transcutaneous bone conduction hearing implants: Systematic review and meta-analysis," *PLoS One*, vol. 14, no. 9, pp. 1–19, 2019, doi: 10.1371/journal.pone.0221484.

[18] H. Taghavi *et al.*, “Technical design of a new bone conduction implant (BCI) system,” *Int. J. Audiol.*, vol. 54, no. 10, pp. 736–744, 2015, doi: 10.3109/14992027.2015.1051665.
[19] H. Taghavi, *The Bone Conduction Implant (BCI) Preclinical Studies, Technical Design and a Clinical Evaluation*. 2014.
[20] S. Reinfeldt, B. Håkansson, H. Taghavi, and M. Eeg-Olofsson, “Bone conduction hearing sensitivity in normal-hearing subjects: Transcutaneous stimulation at BAHA vs BCI position,” *Int. J. Audiol.*, vol. 53, no. 6, pp. 360–369, Jun. 2014, doi: 10.3109/14992027.2014.880813.
[21] J. Gustafsson, “BCDrive TM transducer technology,Cochlear Bone Anchored Solutions, Sweden.” p. 17.
[22] K. Fred, *The Balanced Electromagnetic Separation Transducer for Bone Conduction Audiometry and Hearing Rehabilitation by*. 2017.
[23] B. E. V. Håkansson, “The balanced electromagnetic separation transducer: A new bone conduction transducer,” *J. Acoust. Soc. Am.*, vol. 113, no. 2, pp. 818–825, 2003, doi: 10.1121/1.1536633.
[24] M. R. Goldstein, S. Bourn, and A. Jacob, “Early Osia® 2 bone conduction hearing implant experience: Nationwide controlled-market release data and single-center outcomes,” *Am. J. Otolaryngol. - Head Neck Med. Surg.*, vol. 42, no. 1, 2021, doi: 10.1016/j.amjoto.2020.102818.
[25] R. B. A. Adamson, M. Bance, and J. A. Brown, “A piezoelectric bone-conduction bending hearing actuator,” *J. Acoust. Soc. Am.*, vol. 128, no. 4, pp. 2003–2008, 2010, doi: 10.1121/1.3478778.
[26] H. Liu *et al.*, “Concept and evaluation of a new piezoelectric transducer for an implantable middle ear hearing device,” *Sensors (Switzerland)*, vol. 17, no. 11, 2017, doi: 10.3390/s17112515.
[27] K. Lau *et al.*, “First United Kingdom experience of the novel Osia active transcutaneous piezoelectric bone conduction implant.,” *Eur. Arch. oto-rhino-laryngology Off. J. Eur. Fed. Oto-Rhino-Laryngological Soc. Affil. with Ger. Soc. Oto-Rhino-Laryngology - Head Neck Surg.*, vol. 277, no. 11, pp. 2995–3002, Nov. 2020, doi: 10.1007/s00405-020-06022-7.
[28] M. Goycoolea *et al.*, “Clinical performance of the Osia™ system, a new active osseointegrated implant system. Results from a prospective clinical investigation.,” *Acta Otolaryngol.*, vol. 140, no. 3, pp. 212–219, Mar. 2020, doi: 10.1080/00016489.2019.1691744.
[29] S. Arndt, A. K. Rauch, and I. Speck, “Active transcutaneous bone-anchored hearing implant: how I do it,” *Eur. Arch. Oto-Rhino-Laryngology*, vol. 278, no. 10, pp. 4119–4122, 2021, doi: 10.1007/s00405-021-06946-8.
[30] K.-J. F. Jansson, “A new audiometric bone vibrator, Radioear B81, and the bone conduction implant with emphasis on magnetic resonance imaging,” 2015.
[31] M. Işeri *et al.*, “A new transcutaneous bone anchored hearing device - the Baha® Attract System: the first experience in Turkey.,” *Kulak Burun Bogaz Ihtis. Derg.*, vol. 24, no. 2, pp. 59–64, 2014, doi: 10.5606/kbbihtisas.2014.45143.
[32] Q. Cao, D. Chen, C. Li, Q. Lu, and Y. Zeng, “A Review of the Magnetomechanical Modeling of Magnetostriction Materials,” pp. 2–3, 2014.
[33] B. Carla, “5th Year Internship Report Presented by conducting vibrator for a new generation of bone,” no. 33, 2019.
[34] F. D. Smith, “The magnetostriction constant for alternating magnetic fields,” *Proc. Phys.*

Soc., vol. 42, no. 3, pp. 181–191, 1930, doi: 10.1088/0959-5309/42/3/304.
[35] S. Vinogradov, A. Cobb, and G. Light, "Review of magnetostrictive transducers (MsT) utilizing reversed Wiedemann effect Review of Magnetostrictive Transducers (MsT) Utilizing Reversed Wiedemann Effect," vol. 020008, no. February 2017, 2019, doi: 10.1063/1.4974549.
[36] GeoSci Developers, "Magnetic Permeability," 2018. .
[37] Y. Sakai, S. Karino, and K. Kaga, "Bone-conducted auditory brainstem-evoked responses and skull vibratory velocity measurement in rats at frequencies of 0.5-30 kHz with a new giant magnetostrictive bone conduction transducer," *Acta Otolaryngol.*, vol. 126, no. 9, pp. 926–933, 2006, doi: 10.1080/00016480500536871.
[38] T. Attributes, "Terfenol.pdf."
[39] B. Jones and C. Liang, "Magnetostriction: Revealing the unknown," *IEEE Aerosp. Electron. Syst. Mag.*, vol. 11, no. 3, pp. 3–6, 1996, doi: 10.1109/62.486730.
[40] T. Ueno, H. Miura, and S. Yamada, "Evaluation of a miniature magnetostrictive actuator using Galfenol under tensile stress," *J. Phys. D. Appl. Phys.*, vol. 44, no. 6, pp. 1–5, 2011, doi: 10.1088/0022-3727/44/6/064017.
[41] A. E. Clark, J. B. Restorff, M. Wun-Fogle, T. A. Lograsso, and D. L. Schlagel, "Magnetostrictive properties of body-centered cubic Fe-Ga and Fe-Ga-Al alloys," *IEEE Trans. Magn.*, vol. 36, no. 5 I, pp. 3238–3240, 2000, doi: 10.1109/20.908752.
[42] A. E. Clark, M. Wun-Fogle, J. B. Restorff, and T. A. Lograsso, "Magnetostrictive properties of Galfenol alloys under compressive stress," *Mater. Trans.*, vol. 43, no. 5, pp. 881–886, 2002, doi: 10.2320/matertrans.43.881.
[43] G. R. Popelka, G. Telukuntla, and S. Puria, "Auditory Thresholds by Bone Conduction for High Frequencies," no. Dc, p. 5960.
[44] G. R. Popelka, G. Telukuntla, and S. Puria, "Middle-ear function at high frequencies quantified with advanced bone-conduction measures," *Hear. Res.*, vol. 263, no. 1–2, pp. 85–92, 2010, doi: 10.1016/j.heares.2009.11.002.
[45] D. Messinger and A. Vannas, "Electromechanical Simulation for Transducers in Bone Anchored Hearing Systems," 2020.
[46] "Concept for a magnetoelastic transducer," p. 2019, 2019.
[47] T. Cochlear, "Osia OSI200 Implant," 2005.
[48] O. A. Quaglio, J. Margarida da Silva, E. da Cunha Rodovalho, and L. de Vilhena Costa, "Determination of Young's Modulus by Specific Vibration of Basalt and Diabase," *Adv. Mater. Sci. Eng.*, vol. 2020, p. 4706384, 2020, doi: 10.1155/2020/4706384.
[49] M. Alloy, "Metglas," pp. 1–4, 2011.
[50] M. Al-Shammari and H. Kassab, "Free vibration investigation of isotropic composite skew plate with different shapes holes," vol. 7, pp. 469–474, Oct. 2016.
[51] A. van Casteren, W. Sellers, S. Thorpe, S. Coward, R. Crompton, and R. Ennos, "Factors Affecting the Compliance and Sway Properties of Tree Branches Used by the Sumatran Orangutan (Pongo abelii)," *PLoS One*, vol. 8, p. e67877, Jul. 2013, doi: 10.1371/journal.pone.0067877.
[52] M. Colussi, F. Berto, K. Mori, and F. Narita, "Recent Results on the Brittle Fracture of Terfenol-D Specimens under Magnetic Field," *Am. J. Eng. Appl. Sci.*, vol. 9, no. 4 SE-Research Article, Dec. 2016, doi: 10.3844/ajeassp.2016.1239.1246.
[53] J. J. Scheidler, V. M. Asnani, Z. Deng, and M. J. Dapino, "Dynamic characterization of Galfenol," 2015.
[54] L. Chen, Y. Wang, T. Luo, Y. Zou, and Z. Wan, "The Study of Magnetoimpedance Effect for Magnetoelectric Laminate Composites with Different Magnetostrictive

Layers.,” *Mater. (Basel, Switzerland)*, vol. 14, no. 21, Oct. 2021, doi: 10.3390/ma14216397.